



Contents lists available at ScienceDirect

Deep-Sea Research II

journal homepage: www.elsevier.com/locate/dsr2

The influence of a mature cyclonic eddy on particle export in the lee of Hawaii

Kanchan Maiti^{a,*}, Claudia R. Benitez-Nelson^a, Yoshimi Rii^b, Robert Bidigare^b^a Department of Geological Sciences, University of South Carolina, Columbia, SC 29208, USA^b Department of Oceanography, University of Hawaii, Honolulu, HI 92822, USA

ARTICLE INFO

Article history:

Accepted 3 February 2008

Keywords:

Carbon export
Biogenic silica
Remineralization
Eddies
Thorium-234
North Pacific Subtropical Gyre

ABSTRACT

Mesoscale eddies may enhance primary production (PP) in the open ocean by bringing nutrient-rich deep waters into the euphotic zone, potentially leading to increased transport of particles to depth. This hypothesis remains controversial, however, due to a paucity of direct particle export measurements. In this study, we investigated particle dynamics using ²³⁴Th–²³⁸U disequilibria within a mesoscale cold-core eddy, Cyclone *Opal*, which formed in the lee of the Hawaiian Islands. ²³⁴Th samples were collected along two transects across Cyclone *Opal* as well as during a time-series within the eddy core during a decaying diatom bloom. Particulate carbon (PC), particulate nitrogen (PN) and biogenic silica (bSiO₂) fluxes at 150 m varied spatially and temporally within the eddy and strongly depended on the ²³⁴Th model formulation used (e.g., steady state versus non-steady state, inclusion of upwelling, etc.). Particle fluxes estimated from a steady state model assuming an upwelling rate of 2 m day⁻¹ yielded the best fit to sediment-trap data. These ²³⁴Th-derived particle fluxes ranged from 332 ± 14 to 1719 ± 53 μmol C m⁻² day⁻¹, 27 ± 3 to 114 ± 12 μmol N m⁻² day⁻¹, and 33 ± 20 to 309 ± 73 μmol Si m⁻² day⁻¹. Although PP rates within Cyclone *Opal* were elevated by a factor of 2–3, PC and PN fluxes were the same, within error, inside and outside of Cyclone *Opal*. The ratio of PC export to PP remained surprisingly low at <0.03 and similar to those measured in surrounding waters. In contrast, bSiO₂ fluxes within the eddy core were three times higher. Detailed analyses of ²³⁴Th depth profiles consistently showed excess ²³⁴Th at 100–175 m, associated with the remineralization and possible accumulation of suspended and dissolved organic matter from the surface. We suggest that strong microzooplankton grazing facilitated particulate organic matter recycling and resulted in the export of empty diatom frustules. Thus, while eddies may increase PP, they do not necessarily increase PC and PN export to deep waters. This may be a general characteristic of wind-driven cyclonic eddies of the North Pacific Subtropical Gyre and suggests that eddies may preferentially act as a silica pump, thereby playing an important role in promoting silicic-acid limitation in the region.

© 2008 Elsevier Ltd. All rights reserved.

1. Introduction

Mesoscale eddies are dynamic and ubiquitous features within marine systems (Cheney and Richardson, 1976; Olson, 1980; Falkowski et al., 1991; Allen et al., 1996; McGillicuddy and Robinson, 1997; Dickey et al., 1998; van Haren et al., 2006). Recent evidence suggests that in the open-ocean, these episodic phenomena enhance the upwelling of cold, nutrient-rich deep waters into the euphotic zone, thereby increasing primary production (PP), potentially altering plankton community structure, and facilitating carbon export in otherwise nutrient-deficient waters (Garcon et al., 2001; Sweeney et al., 2003; McGillicuddy et al., 2007). Current estimates suggest that 10–50% of global new

PP is caused by eddy-induced nutrient fluxes (Falkowski et al., 1991; McGillicuddy et al., 1998; Oschlies and Garcon 1998; Siegel et al., 1999; Letelier et al., 2000). Such a wide range in estimates is due to the paucity of direct field observations of eddy biogeochemistry (Savidge and Williams, 2001; Bidigare et al., 2003). The ephemeral nature of most eddies, coupled with their spatial and temporal variability, makes them difficult to predict and study. Eddy dynamics constitute a further confounding factor, particularly with regard to biological community structure and resulting particle formation and export, which likely vary with eddy age (e.g., Flierl and McGillicuddy, 2002; Haury et al., 1978; Haury, 1984; Woods 1988; Dower and Denman, 2001; Sweeney et al., 2003).

Wind-induced cold-core cyclonic eddies are conspicuous oceanographic features that occur off the leeward shores of the Hawaiian Islands throughout the year, but most frequently during periods of high trade wind intensity (October–March) (Patzel, 1969; Lumpkin, 1998; Chavanne et al., 2002; Dickey et al., 2008). These features are characterized by divergent flow at the surface

* Corresponding author. Present address: Marine Chemistry and Geochemistry, Woods Hole Oceanographic Institution, 266 Woods Hole Road, Woods Hole, MA 02543, USA. Tel.: +1508 289 3916.

E-mail address: kmaiti@whoi.edu (K. Maiti).

that produces localized upwelling of cooler, nutrient-rich deep waters (Olaizola et al., 1993). Hawaiian lee eddies tend to be of significant size (~180 km in diameter) and have a typical life-span of 3–8 months (Patzel, 1969; Lumpkin, 1998). Their regular formation provides a natural laboratory for investigating eddy-enhanced biological production and carbon export in an accessible subtropical oligotrophic setting.

Although few in number, several previous studies suggest that Hawaiian lee eddies are highly productive features. For example, Falkowski et al. (1991) sampled a 1-month-old cyclonic eddy off the coast of Hawaii in August 1989 and found a ~3.5-fold increase in PP relative to the adjacent ocean. Most of the PP increase was attributed to the influx of 'new' nitrate into the system from depth, with the ratio of nitrate-based to total production (*f*-ratio), increasing from 0.2 in surrounding waters to 0.8 within the eddy (Allen et al., 1996). Subsequent studies of other cold-core Hawaiian lee eddies have also found significant increases in PP, plankton biomass, and larger organisms, such as the Pacific blue marlin (Seki et al., 2001; Bidigare et al., 2003).

In this study, the disequilibrium between ^{234}Th and its parent, ^{238}U was used to quantify the export of particles derived from a biologically mature eddy, Cyclone *Opal*. ^{234}Th is produced by the radioactive decay of ^{238}U ($t_{1/2} = 4.47 \times 10^9$ years). Since ^{234}Th is highly particle reactive and has a half-life of 24.1 days, the disequilibrium between its soluble parent, ^{238}U , and the measured ^{234}Th activity provides an estimate of the net rate of particle export from the upper ocean on time scales of days to weeks (Buesseler, 1998). Thus ^{234}Th enables one to examine particle export over the preceding 4–6 weeks, allowing us to examine particle fluxes that have taken place since eddy formation.

2. Methods

2.1. Study site and sample collection

Cyclone *Opal* was sampled from March 10–28, 2005 (E-Flux III) on board the R/V *Wecoma* in the lee of the island of Hawaii (Fig. 1A, also see Dickey et al., 2008). Cyclone *Opal* appeared in moderate resolution imaging spectroradiometer (MODIS) and geostationary operational environmental satellites (GOES) imagery between February 18 and 25, 2005 at approximately 20.30°N, 156.30°W, southwest of the 'Alenuihaha Channel (Nencioli et al., 2008). Spanning ~220 km, Cyclone *Opal* moved rapidly southward by ~165 km during the sampling period with an overall average displacement speed of ~8 km d⁻¹. This fast movement, coupled with the small ~40 km size of the eddy core (characterized by enhanced biomass, and shallow mixed-layer depth (MLD)) made sampling difficult (Fig. 1A). Samples across Cyclone *Opal* from E-Flux III Transect 3 (herein referred to as ^{234}Th sampling Transect 1) were collected on March 13, 2005, when the approximate location of the eddy-center was between stations EF-18 and EF-21 (Fig. 1B). The shoaling of the isopycnal lines is used here as a direct reflection of upwelling intensity (Fig. 2). The gradual deepening of isopycnal lines is indicative of the decrease in upwelling intensity from the center towards the eddy edge. Sampling during E-Flux III Transect 6 (herein referred to as ^{234}Th sampling Transect 2) was conducted on March 22, 2005 from within the center of the eddy towards the surrounding waters (Fig. 1B). Time-series ^{234}Th sampling within the eddy core was conducted over a 6-day period from March 16–21, 2005 (IN stations). Both *in situ* measurements (ADCP, SST, MLD) and satellite imagery suggested that sampling was maintained within the eddy core during the course of the time-series measurements (Dickey et al., 2008). Control or OUT stations were sampled to the west of the island of Maui, in a region well removed from the eddy flow field (Fig. 1B).

Profiles of total ^{234}Th were collected from 21 separate casts using a CTD rosette with 10-L Niskin-like bottles. Sample depths ranged from 0 to 400 m during the transects, and from 0 to 1000 m at each IN and OUT station. Samples for particulate ^{234}Th , particulate carbon (PC), particulate nitrogen (PN), and biogenic silica (bSiO₂) were collected with a large-volume, *in situ* pump deployed below the mixed layer at 150 m. Pump samples consisted of ~300 L of seawater passed at 7 L min⁻¹ sequentially through 142-mm-diameter 53- and 10- μm mesh nitex screens, followed by a 1- μm pore size micro-quartz filter (QMA). Nitex screens were rinsed onto 25-mm-diameter silver filters and the entire sample was analyzed for PC, PN, and bSiO₂ after ^{234}Th analysis. Additional samples were collected using particle interceptor sediment traps (PITs) deployed for a minimum of 3 days inside and outside of the eddy at 150 m following the methods described by Karl et al. (1991) and Rii et al. (2008). The majority (~1.75 L) of three separate sediment-trap sample tubes were filtered onto 25-mm GF/F pre-combusted filters for PC and PN analyses. A portion of the remaining three sediment-trap tubes (250 mL) were combined and filtered onto 25-mm 0.8- μm polycarbonate membranes for bSiO₂. Three blanks (2 L of the unused brine fill solution) were filtered using the exact same method.

2.2. ^{234}Th analyses

All sediment-trap samples used for PC and PN analysis were directly counted for ^{234}Th activity using the methods described by Buesseler et al. (1995). All water-column total ^{234}Th samples were processed using the 4-L manganese oxide co-precipitation technique described in detail by Pike et al. (2005) and Rutgers van der Loeff et al. (2006). *In situ* pump samples were collected and processed according to the techniques described by Buesseler et al. (1998, 2001, 2005). All particulate and total ^{234}Th samples were counted directly on a five sample gas-flow proportional low-level RISØ beta counter for at least 12 h or until counting errors were < 3%. Samples were then recounted after > 150 days (~6 half lives) since collection to precisely determine background count rates, which averaged 0.51 ± 0.05 cpm. The detector was calibrated for each cruise with > 3000 m deep-water samples (assumed to be in radioactive equilibrium), collected from five different bottles within a cast ($n = 3$). Replicate deep-water samples varied by less than 5% between casts and other E-Flux cruises. Detector calibration for the stacked QMA and particulate samples was determined by using known ^{234}Th activities in the same sample geometries (Buesseler et al., 1998, 2001). After recounting samples for background activities, total ^{234}Th samples were purified using ion exchange chemistry. Recovery of the added ^{230}Th yield monitor was quantified by inductively coupled plasma-mass spectroscopy with addition of a ^{229}Th internal standard (Pike et al., 2005; Rutgers van der Loeff et al., 2006). Corrections were applied to ^{234}Th activities based on the ^{230}Th recovery for each sample, which averaged 0.89 ± 0.06 . All data are decay corrected to the time of collection and reported with a propagated error that includes uncertainties associated with sampling, counting, and other calibration errors.

2.3. PC, PN and bSiO₂ analyses

Following ^{234}Th analysis, sediment-trap and pump sample filters were analyzed for PC and PN using a Perkin-Elmer CHN analyzer according to the Hawaii Ocean Time-series (HOT) protocol, which does not include fuming with HCl or distilled water rinsing pretreatments (Karl et al., 1991). The 25-mm silver filter samples were weighed, cut in half, and reweighed, with half

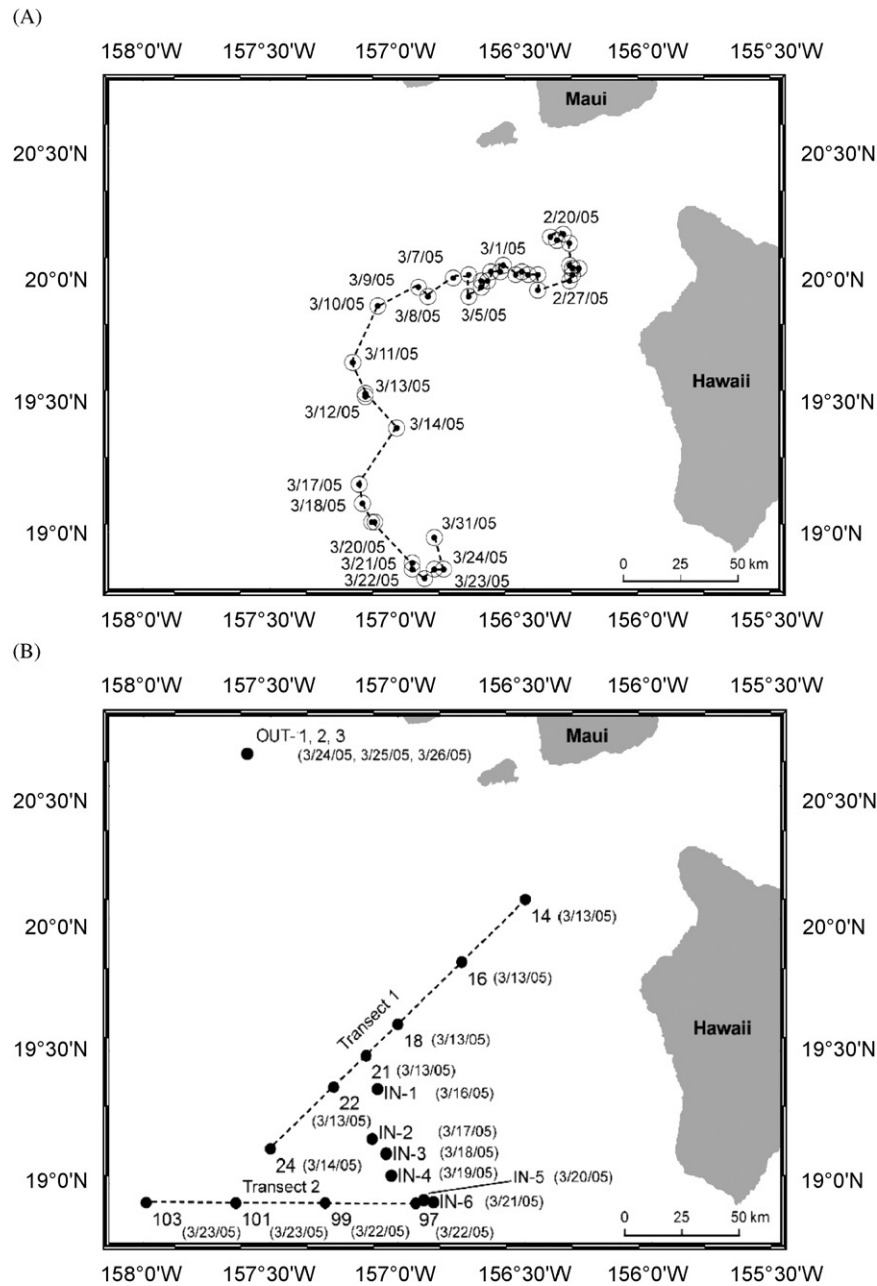


Fig. 1. (A) Spatial and temporal location of the eddy center as derived from GOES SST imagery prior to March 10th (courtesy of Carrie Leonard), and thereafter using shipboard SST and ADCP (Dickey et al., 2008). (B) Location of ^{234}Th sampling stations from where ^{234}Th samples were collected.

of the filter analyzed for PC and PN. The 142-mm QMA pump filters were subsampled into 8-mm-diameter circles using a stainless steel cutter. A set of three 8-mm circles were then combined and three sets were analyzed for PC and PN. The remaining half of the silver filters were cut into quarters and reweighed. bSiO_2 was then extracted from the duplicate (1/4) silver filters following the Na_2CO_3 digestion method outlined by DeMaster (1981) and dissolved Si measured by Hansen and Koroleff (1999). bSiO_2 was not measured on the QMA filters from the *in situ* pumps because of the high Si blanks associated with these filters.

2.4. Calculating ^{234}Th -based particle flux

The export flux of ^{234}Th at a particular oceanic depth can be estimated by solving the following activity balance equation for

total ^{234}Th in the ocean (Buesseler et al., 1992; Cochran et al., 1995; Savoye et al., 2006):

$$\frac{\delta A_{\text{Th}}}{\delta t} = A_{\text{U}}\lambda_{\text{Th}} - A_{\text{Th}}\lambda_{\text{Th}} - P_{\text{Th}} + V, \quad (1)$$

where $\delta A_{\text{Th}}/\delta t$ is the non-steady state (NSS) term and reflects changes in total ^{234}Th activity with time, A_{U} is the ^{238}U activity determined from salinity (^{238}U dpm $\text{L}^{-1} = 0.0686 \times \text{salinity} \times \text{density}$; Chen et al., 1986), A_{Th} is the measured activity of total ^{234}Th , λ_{Th} is the decay constant for ^{234}Th ($= 0.0288 \text{ d}^{-1}$), P_{Th} is the net removal flux of ^{234}Th on particles, and V represents the sum of advective and diffusive processes (Buesseler et al., 1992; Savoye et al., 2006). In most open-ocean regimes, steady state (SS) is assumed ($\delta A_{\text{Th}}/\delta t = 0$) and advection and diffusion considered minimal ($V = 0$) (Savoye et al., 2006). Within wind-driven cyclonic eddies, however, both of these assumptions need to be tested.

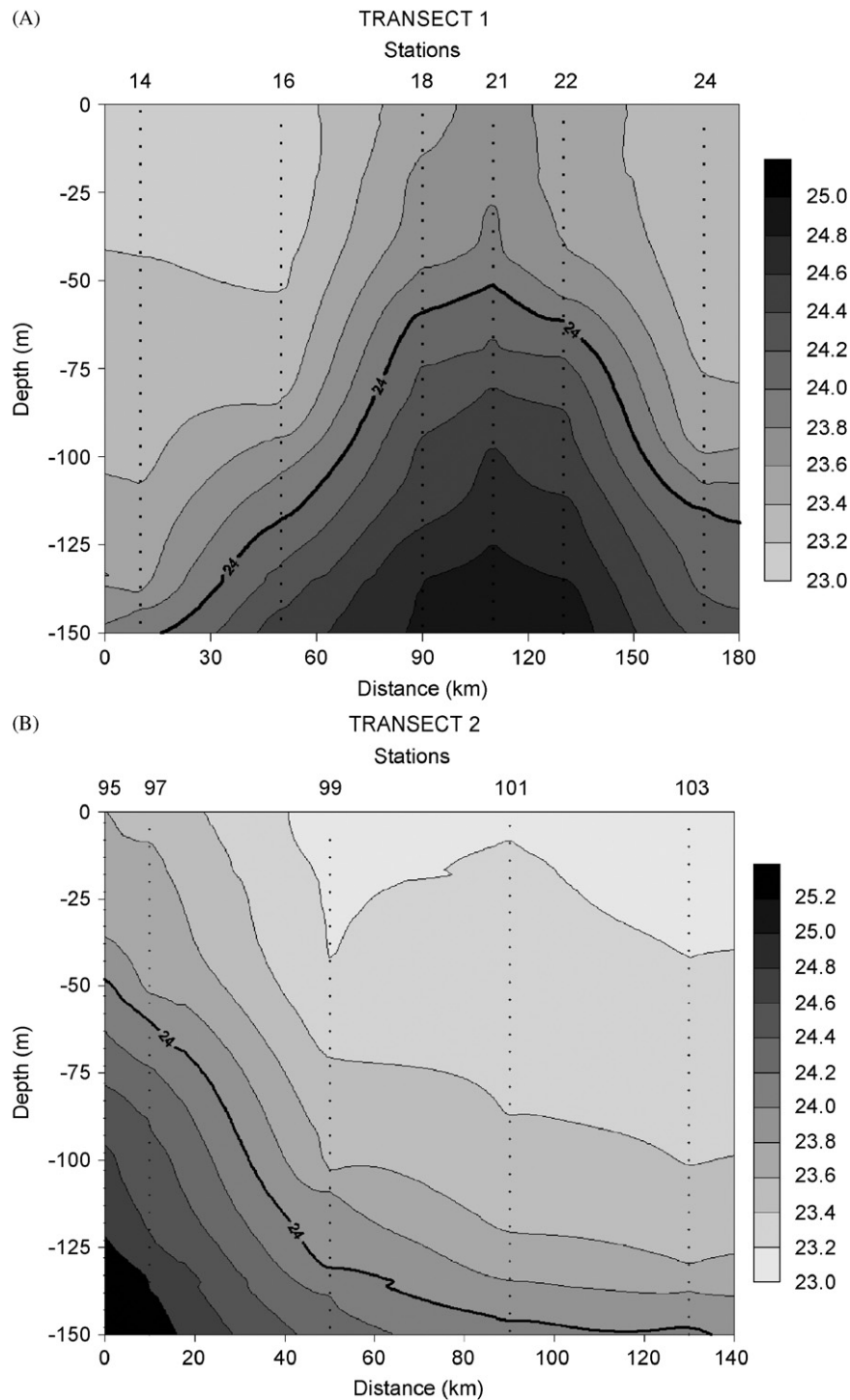


Fig. 2. Depth versus density profile of the water-column along (A) Transect 1 and (B) Transect 2. The bold line represents the $\sigma_T = 24 \text{ kg m}^{-3}$ isopycnal density surface with contour intervals of 0.2σ .

Upwelling is a significant process, at least during initial eddy formation. Once the eddy is removed from the wind driven flow field, vertical velocities should decrease to near negligible values (Nencioli et al., 2008). Within Cyclone *Opal*, physical measurements suggest that the eddy remained a closed system above the upper 70 m prior to measurement (Nencioli et al., 2008). Below 70 m, however, Nencioli et al. (2008) suggest that Cyclone *Opal* may have behaved as an open system, with continuous exchange between deeper waters, particularly over the time period when Cyclone *Opal* moved rapidly south (March 11–13). Upwelling of ^{234}Th -rich deep

waters would result in a decrease in the absolute deficiency of ^{234}Th relative to ^{238}U . In other words, the calculated export flux of ^{234}Th from the water-column would be underestimated (Savoie et al., 2006). To test the effect of vertical advection, or upwelling, Eq. (1) was rewritten as follows, assuming SS:

$$P_{\text{Th}} = \lambda_{\text{Th}}(A_{\text{U}} - A_{\text{Th}}) + w \frac{\partial A_{\text{Th}}}{\partial z}, \quad (2)$$

where w is the upwelling velocity and $\partial A_{\text{Th}}/\partial z$ is the vertical gradient in ^{234}Th activity. The vertical ^{234}Th gradient, $\partial A_{\text{Th}}/\partial z$, is

estimated from the ^{234}Th activity within a given layer and the activity from the base of this layer (Buesseler et al., 1995; Murray et al., 1996; Bacon et al., 1996). No other physical mixing terms (e.g., horizontal advection and diffusion or vertical diffusion) were included.

During the time-series occupation of Cyclone *Opal*, there was a significant decrease in chlorophyll *a* (chl *a*) concentrations and a rapid transition in community structure from diatoms to smaller organisms (Brown et al., 2008; Rii et al., 2008), suggesting that the system was not in SS. Therefore, temporal changes in ^{234}Th activity must also be included ($\delta A_{\text{Th}}/\delta t$ in Eq. (1)), as a negative NSS term results in an overestimation of the ^{234}Th flux and vice versa.

In this study, we tested three models for determining the ^{234}Th flux within Cyclone *Opal*: (1) SS and no physical effects ($\delta A_{\text{Th}}/\delta t = V = 0$), (2) SS and the inclusion of upwelling ($w\partial A_{\text{Th}}/\partial z$), and (3) NSS ($\delta A_{\text{Th}}/\delta t \neq 0$) and no physical effects ($V = 0$). We also tested a fourth method for determining ^{234}Th fluxes that is based on the ^{234}Th directly measured within sediment traps as opposed to the ^{234}Th : ^{238}U disequilibria measured in the water-column (i.e., model 1). An important distinction between the water-column and the sediment-trap-derived ^{234}Th fluxes is the time scale over which these two types of measurements pertain. While the former represents a flux integrated over a time interval of 4–6 weeks, the latter represents the flux integrated only over the time period in which the sediment traps are deployed (days). Furthermore, upper-ocean sediment traps have been known to suffer from artifacts associated with hydrodynamic effects causing them to both over- and under-collect sinking material (Buesseler, 1991; Buesseler et al., 2007).

Once the ^{234}Th flux is determined, the export flux of PC, PN, bSiO_2 or any other constituent can be calculated by using the empirical relationship between a given constituent, X, and particulate ^{234}Th as follows:

$$(P_X)_z = (P_{\text{Th}})_z \times \left(\frac{X}{^{234}\text{Th}} \right)_{iz} \quad (3)$$

Here $(P_{\text{Th}})_z$ is the depth integrated ^{234}Th flux to the lower boundary depth, “z”, and $(X/^{234}\text{Th})_{iz}$ is the X/ ^{234}Th ratio measured in sinking particles of size “i” and collected at depth “z”. $(P_X)_z$ is thus the particle flux of a given element X. The key is to measure the X/ ^{234}Th at the base of the depth interval of interest and to use it with the integrated ^{234}Th disequilibrium flux data determined over the same depth interval (Buesseler et al., 2006; Benitez-Nelson and Charette, 2004). For the present study, all export fluxes are calculated at 150 m to compare with sediment traps and the particle fluxes measured at the nearby HOT site (Karl et al., 1996). The elemental ratios of PC, PN and bSiO_2 to ^{234}Th are derived from size-fractionated samples collected by large volume *in situ* pumps and sediment traps deployed at 150 m. Due to time constraints, pump samples were only collected from Transect 2 and IN and OUT stations.

3. Results

3.1. Transects ^{234}Th

Total ^{234}Th activities varied both with depth and station location and ranged from 1.93 to 2.75 dpm L^{-1} . In general, largest ^{234}Th : ^{238}U disequilibria occurred in the upper 100 m, coincident with the depth of the deep total chl *a* maximum (DCM), suggesting that this region was where particle formation and sinking rates were highest. Activities greater than secular equilibrium were typically found at 150–200 m and were attributed to particle remineralization. During Transects 1 and 2,

samples were collected along the isopycnal density surface of $\sigma_T = 24.0 \text{ kg m}^{-3}$ as it followed the MLD most closely, which varied from 130 to 26 m during Transect 1 and from 56 to 130 m during Transect 2. Here, MLD is defined as the depth at which seawater temperature is 1 °C less than the temperature at 10 m, following the convention used in Benitez-Nelson et al. (2007) and other companion papers (e.g., Dickey et al., 2008; Nencioli et al., 2008). Although above the depth of the DCM, typically located between $\sigma_T = 24.2$ and 24.4 kg m^{-3} (Rii et al., 2008), there is an excellent correlation between ^{234}Th deficiency (^{238}U – ^{234}Th) and the $^{234}\text{Th}/^{238}\text{U}$ ratio with the $\sigma_T = 24.0 \text{ kg m}^{-3}$ isopycnal surface during both transects (Transect 1: $r^2 = 0.90$, $p < 0.001$; Transect 2: $r^2 = 0.95$, $p < 0.001$, Fig. 3). This suggests that ^{234}Th scavenging increases with the shoaling of isopycnals and associated influx of nutrients into the euphotic zone.

^{234}Th fluxes along each transect were determined over the upper 150 m using Eq. (1) and assuming SS and ignoring physical processes, such as advection and diffusion. Maximum ^{234}Th export fluxes along Transect 1 occurred at Station EF-16 ($1432 \pm 156 \text{ dpm m}^{-2} \text{ d}^{-1}$) followed by Station EF-18 ($1050 \pm 140 \text{ dpm m}^{-2} \text{ d}^{-1}$), with the other stations generally having ^{234}Th fluxes similar in magnitude to those measured at the OUT Stations (Fig. 4A, Table 1). These high fluxes were to the northeast of the eddy core located at EF-21 (as identified by shallowing of the $\sigma_T = 24.0 \text{ kg m}^{-3}$ isopycnal surface), and may be due to eddy movement prior to sampling. The center of Cyclone *Opal* remained situated for several weeks in close proximity to EF-16 and EF-18, before moving rapidly southward during Transect 1 sampling. While the $\sigma_T = 24.0 \text{ kg m}^{-3}$ records the instantaneous center of the eddy, ^{234}Th : ^{238}U disequilibria integrates over several weeks. Therefore, higher fluxes to the north of the eddy core may reflect an earlier export event and is consistent with the leaky bottom hypothesis proposed by Nencioli et al. (2008) who suggested that an export signature may have been left behind in the wake of the eddy based on low oxygen and chl *a* concentrations. During Transect 2, there is a gradual decrease in ^{234}Th export from the center of Cyclone *Opal*, Station EF-97 ($931 \pm 136 \text{ m}^{-2} \text{ d}^{-1}$) towards surrounding waters, Station EF-103 ($149 \pm 100 \text{ dpm m}^{-2} \text{ d}^{-1}$) (Fig. 4B).

3.2. Process station time-series ^{234}Th

Six water-column ^{234}Th profiles were collected over a period of 1 week (March 16–21) within the center of Cyclone *Opal*. Total ^{234}Th activities varied both temporally and spatially, ranging from 1.97 to 2.82 dpm L^{-1} . Similar to the transects, largest ^{234}Th : ^{238}U disequilibria typically occurred in the upper 100 m while activities greater than secular equilibrium were found at 100–175 m due to particle remineralization and possible accumulation of dissolved and particulate organic matter from surface waters. We used the four approaches discussed in Section 2.4 to determine the ^{234}Th flux at 150 m and assess the underlying assumptions of SS and the effects of advection and diffusion.

Assuming SS and ignoring advection and diffusion, we calculated the ^{234}Th flux at 150 m using total water-column ^{234}Th activities measured at all six IN stations. Fluxes varied substantially with time, ranging from 237 to 1141 $\text{dpm m}^{-2} \text{ d}^{-1}$ with an average flux of $590 \pm 295 \text{ dpm m}^{-2} \text{ d}^{-1}$ (Fig. 5). For comparison, the average flux of ^{234}Th estimated using the ^{234}Th captured in the sediment traps deployed during the first five IN stations was significantly higher, $1028 \pm 48 \text{ dpm m}^{-2} \text{ d}^{-1}$.

In most ^{234}Th flux calculations, physical transport processes are often assumed to be negligible. However, cyclonic mesoscale eddies have significant upwelling within the eddy center, at least during initial formation. As a result, a sensitivity test was

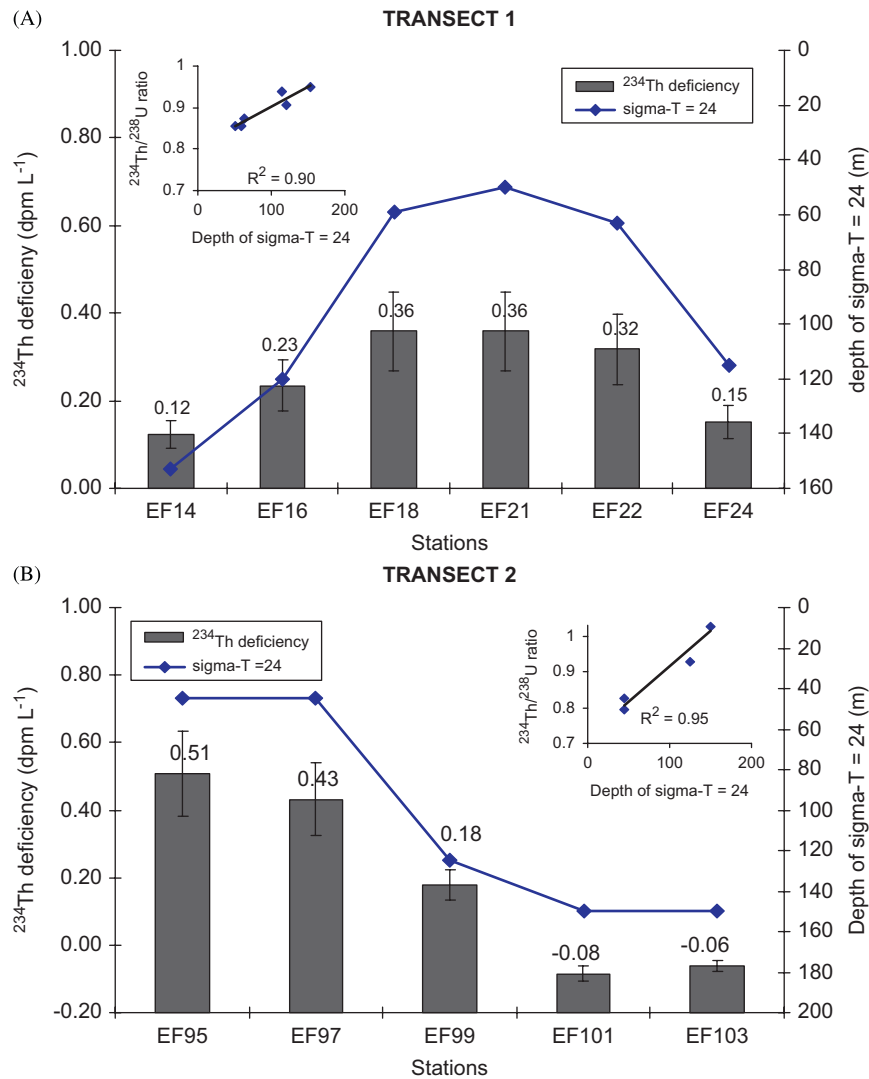


Fig. 3. Deficiency of ^{234}Th along the $\sigma\text{-T} = 24.0 \text{ kg m}^{-3}$ isopycnal for (A) Transect 1 and (B) Transect 2. Note the significant correlations between the depth of $\sigma\text{-T} = 24.0 \text{ kg m}^{-3}$ and the $^{234}\text{Th}/^{238}\text{U}$ ratio.

conducted in order to understand the effect of continuous upwelling on ^{234}Th export fluxes. Dickey et al. (2008) used the spatial wind vector field distribution derived from QuikScat data collected during E-Flux III to compute upwelling and downwelling velocities via Ekman pumping. They found that during trade wind conditions, strong upwelling patterns are generated with values reaching a maximum of $1.5\text{--}2.5 \text{ m d}^{-1}$ just downwind of the 'Alenuihaha Channel, where the formation of Hawaiian lee eddies typically occurs. Therefore, we used upwelling velocities of 1.0, 2.0, and 3.0 m d^{-1} to determine the effect of upwelling on the ^{234}Th fluxes within the core of Cyclone *Opal*. Assuming that the upwelling intensity remained the same for all six IN stations and that there is negligible horizontal advection (which is probably true for eddy center), we determined that ^{234}Th export fluxes increased by as much as five-fold, depending on the upwelling velocity used (Table 1). This effect is most pronounced for IN-4 and is minimal for IN-6, due to changes in the vertical depth gradient of ^{234}Th . The average ^{234}Th fluxes for all six IN stations are 828 ± 450 , 1092 ± 617 and $1356 \pm 804 \text{ dpm m}^{-2} \text{ d}^{-1}$ for upwelling velocities of 1, 2, and 3 m d^{-1} , respectively. An upwelling velocity of 2 m d^{-1} results in a ^{234}Th flux of similar magnitude to that directly measured in the sediment-trap, which is $1028 \pm 48 \text{ dpm m}^{-2} \text{ d}^{-1}$.

In order to understand the influence of the NSS term ($\delta A_{\text{Th}}/\delta t$), we first calculated the depth-weighted average total ^{234}Th activities (dpm L^{-1}) over the upper 150 m for all IN stations (Fig. 6). Average ^{234}Th activities show no significant change over time (within errors) from IN-1 to IN-4. After IN-4, however, there is a substantial decrease in ^{234}Th activity, probably in response to the decrease in chl *a* concentration between IN-3 and IN-4 (Fig. 7A). To calculate the NSS component across the transition from IN-4 to IN-5, we separated the time-series sampling into two time periods: the average ^{234}Th activity from IN-1 to IN-4 ($2.40 \pm 0.03 \text{ dpm L}^{-1}$) and the average ^{234}Th activity from IN-5 to IN-6 ($2.26 \pm 0.07 \text{ dpm L}^{-1}$). The NSS component was calculated to be $6600 \pm 3600 \text{ dpm m}^{-2} \text{ d}^{-1}$, substantially larger than the average SS, no upwelling model flux of $376 \pm 125 \text{ dpm m}^{-2} \text{ d}^{-1}$ determined over IN-1 to IN-4, and the average flux of $942 \pm 282 \text{ dpm m}^{-2} \text{ d}^{-1}$ over IN-5 and IN-6. Although this exercise stresses the importance of the NSS term in particle flux models, the large errors associated with this calculation ($>50\%$ error associated with NSS term) and the sensitivity of the NSS model to short time periods (days), suggested that the NSS model could not be meaningfully used in the present study. A similar conclusion was reached by Savoye et al. (2006), who suggested that stations should only be reoccupied after a delay of at least 1–2 weeks to

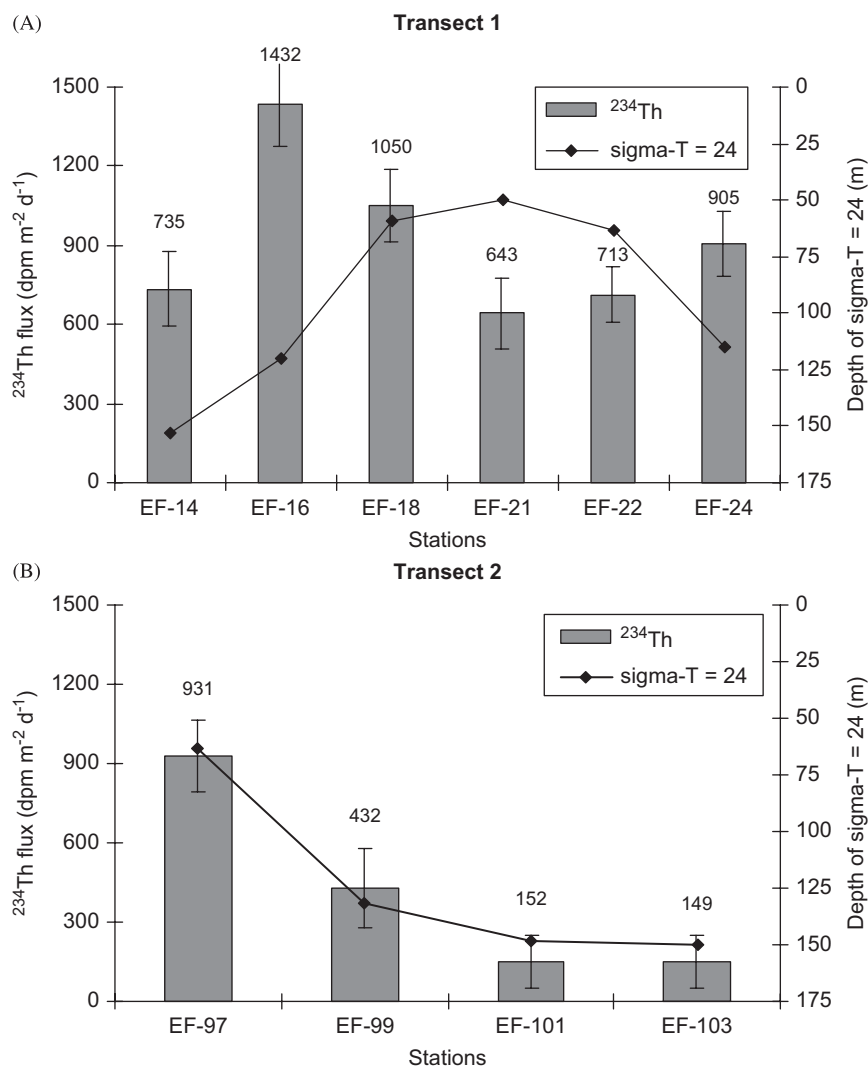


Fig. 4. ^{234}Th -derived fluxes at 150 m using a SS model and assuming no physical processes for (A) Transect 1 and (B) Transect 2.

minimize model sensitivity and to avoid issues associated with patchiness that often occur during plankton blooms. Thus the present scenario highlights the importance of reoccupying stations and the limitation of assuming a SS model when the NSS component may be the largest term in Eq. (1).

3.3. Variability in PC (PN and bSiO_2)/ ^{234}Th ratio

In order to translate ^{234}Th fluxes into PC, PN and bSiO_2 export, the PC (and PN and bSiO_2)/ ^{234}Th ratio of the sinking particles must be measured. In this study, *in situ* pump samples were collected at 150 m depth using three different size fractions from each station along Transect 2 and at all IN and OUT stations (Table 2). sediment-trap PC (and PN and bSiO_2)/ ^{234}Th ratios were only obtained at IN and OUT stations. Along Transect 2, the $\text{C}/^{234}\text{Th}$ ratios on the $\geq 53\text{-}\mu\text{m}$ size fraction showed a gradual decrease from $1.97 \pm 0.06 \mu\text{mol C dpm}^{-1}$ as one moved from the center of Cyclone *Opal* to the outer edge. The $\text{bSiO}_2/^{234}\text{Th}$ ratio showed a similar trend, decreasing from 0.33 ± 0.07 to $0.10 \pm 0.02 \mu\text{mol Si dpm}^{-1}$. For the six IN stations, the $\text{C}/^{234}\text{Th}$ ratio on the $\geq 53\text{-}\mu\text{m}$ fraction varied from 1.22 to $1.88 \mu\text{mol C dpm}^{-1}$, which is similar to the average $\text{C}/^{234}\text{Th}$ ratio of $1.50 \pm 0.04 \mu\text{mol dpm}^{-1}$ measured within the sediment traps, suggesting that the large particles sampled with the pumps

are representative of sinking particles. The $\text{C}/^{234}\text{Th}$ ratio observed in the 1- to 10- μm and <1- μm size fractions are for the most part lower than the $\geq 53\text{-}\mu\text{m}$ size fraction (Fig. 7B; Table 2). This trend is similar to that observed at HOT (Benitez-Nelson et al., 2001) and the Arabian Sea (Buesseler et al., 1998).

The PC (and N and bSiO_2)/ ^{234}Th ratios of different size fractions collected by the *in situ* pump at 150 m show large temporal variability (Fig. 7B–D), with PC (and PN and bSiO_2)/ ^{234}Th ratios varying the most in the large, $\geq 53\text{-}\mu\text{m}$ size class, where community changes were greatest (Fig. 7B and C; Table 2). No clear trends in elemental/ ^{234}Th ratios with time or ^{234}Th flux were observed despite rapid changes in community structure associated with an 80% decrease in diatom biomass (Fig. 7A; Rii et al., 2008; Brown et al., 2008). On average, the $\text{bSiO}_2/^{234}\text{Th}$ ratio on the $\geq 53\text{-}\mu\text{m}$ size particles within Cyclone *Opal* was $\sim 15\%$ higher (0.22 ± 0.06) than in surrounding waters (0.19 ± 0.02), whereas the PC (and PN)/ ^{234}Th ratio remained the same (Table 2).

Microscope images of sediment-trap material indicate that the particle flux was dominated by empty frustules of large centric and smaller pennate diatoms, consistent with the rapid decline in diatom biomass observed in the surface waters (Rii et al., 2008; Brown et al., 2008). As a result the bSiO_2/C molar ratio of trap material decreased by a factor of 3, from 0.28 ± 0.02 to 0.07 ± 0.01 inside versus outside the eddy (Rii et al., 2008).

Table 1
Measured and modeled ^{234}Th fluxes for all stations

Station	^{234}Th flux (no upwelling) ($\text{dpm m}^{-2} \text{d}^{-1}$)	^{234}Th flux (1 m d^{-1} upwelling) ($\text{dpm m}^{-2} \text{d}^{-1}$)	^{234}Th flux (2 m d^{-1} upwelling) ($\text{dpm m}^{-2} \text{d}^{-1}$)	^{234}Th flux (3 m d^{-1} upwelling) ($\text{dpm m}^{-2} \text{d}^{-1}$)
Transect 1				
EF-14	735 ± 142			
EF-16	1432 ± 156			
EF-18	1050 ± 140			
EF-21	643 ± 135			
EF-22	713 ± 106			
EF-24	905 ± 125			
Center				
IN-1	529 ± 139	1041 ± 273	1554 ± 408	2067 ± 543
IN-2	322 ± 146	403 ± 184	485 ± 221	566 ± 255
IN-3	414 ± 147	519 ± 181	625 ± 220	730 ± 259
IN-4	237 ± 110	583 ± 314	930 ± 514	1276 ± 753
IN-5	1142 ± 140	1623 ± 198	2104 ± 257	2585 ± 317
IN-6	742 ± 147	799 ± 158	855 ± 169	912 ± 181
Average IN	564 ± 333	828 ± 450	1092 ± 617	1356 ± 804
Sediment- trap	1028 ± 48			
Transect 2				
EF-97	931 ± 136			
EF-99	432 ± 150			
EF-101	152 ± 101			
EF-103	149 ± 100			
OUT				
OUT-1	517 ± 156			
OUT-3	526 ± 165			
OUT-3	534 ± 161			
Sediment- trap	525 ± 34			

Note that no ^{234}Th profiles were collected at IN-7.

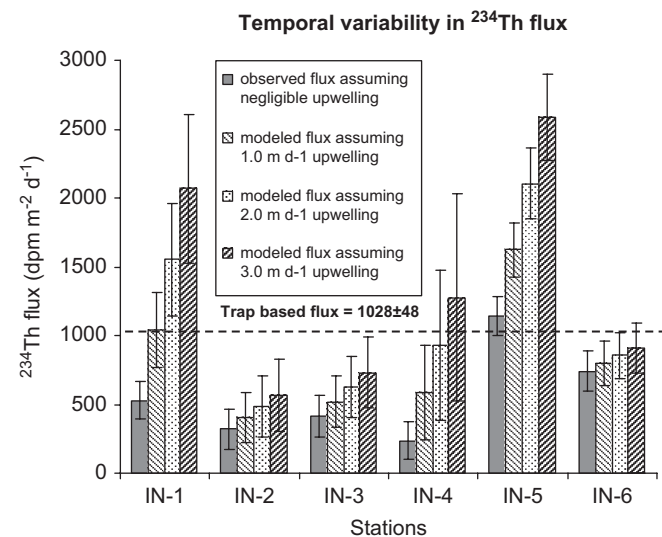


Fig. 5. Variability in ^{234}Th flux at the eddy center using a NSS model with upwelling rates ranging from 0 to 3 m d^{-1} .

The bSiO_2/C ratio for $\geq 53\text{-}\mu\text{m}$ samples collected via the *in situ* pumps increased from 0.11 ± 0.02 to 0.18 ± 0.04 towards the end of the time-series, with an average bSiO_2/C ratio of 0.15 ± 0.03 . Outside Cyclone *Opal*, the average bSiO_2/C ratio for $\geq 53\text{-}\mu\text{m}$ pump samples is a factor of 2 lower, 0.08 ± 0.01 . This is not surprising given the fact that large diatoms comprised most of the biomass observed at the eddy center, whereas communities at the

OUT stations were dominated (>80%) by smaller autotrophs (<10 μm cells), such as prymnesiophytes, pelagophytes and *Prochlorococcus* spp.

3.4. PC, PN and bSiO_2 fluxes

During Transect 2, the SS flux of PC, PN, and bSiO_2 , decreased from $1837 \pm 274 \mu\text{mol C m}^{-2} \text{d}^{-1}$, $145 \pm 26 \mu\text{mol N m}^{-2} \text{d}^{-1}$, and $306 \pm 76 \mu\text{mol Si m}^{-2} \text{d}^{-1}$ at the core of Cyclone *Opal* to $207 \pm 139 \mu\text{mol C m}^{-2} \text{d}^{-1}$, $18 \pm 11 \mu\text{mol N m}^{-2} \text{d}^{-1}$, and $14 \pm 9 \mu\text{mol Si m}^{-2} \text{d}^{-1}$ in surrounding waters (Fig. 8, Table 3). For the six IN stations at the eddy center, PC, PN and bSiO_2 fluxes over the upper 150m were determined using both the PC (PN and bSiO_2)/ ^{234}Th of the $\geq 53\text{-}\mu\text{m}$ size fraction and the PC (PN and bSiO_2)/ ^{234}Th ratio determined from the sediment traps. The PC export flux determined using the pump samples and the water-column-derived ^{234}Th export ranged from 332 ± 196 to $1719 \pm 217 \mu\text{mol C m}^{-2} \text{d}^{-1}$ (Fig. 9), with an average of $968 \pm 570 \mu\text{mol C m}^{-2} \text{d}^{-1}$ for all five IN stations (assuming no upwelling), similar to the $886 \pm 444 \mu\text{mol C m}^{-2} \text{d}^{-1}$ calculated using the sediment-trap PC/ ^{234}Th ratio (Fig. 10). This is substantially less, however, than the PC fluxes determined directly from the sediment traps of $1544 \pm 112 \mu\text{mol C m}^{-2} \text{d}^{-1}$. When upwelling rates of 1 and 2 m d^{-1} are included in the water-column-derived ^{234}Th fluxes, PC fluxes increase to an average value of 1357 ± 584 and $1726 \pm 758 \mu\text{mol C m}^{-2} \text{d}^{-1}$, respectively. At the OUT stations, water-column ^{234}Th and sediment-trap-derived PC fluxes are calculated to be 845 ± 85 and $1522 \pm 201 \mu\text{mol C m}^{-2} \text{d}^{-1}$, respectively (Fig. 10, Table 3).

The modeled PN export flux varies between 27 ± 16 and $114 \pm 18 \mu\text{mol N m}^{-2} \text{d}^{-1}$ (Fig. 9), with an average of $66 \pm 38 \mu\text{mol N m}^{-2} \text{d}^{-1}$ for all five IN stations (assuming no upwelling), again similar to the $85 \pm 43 \mu\text{mol N m}^{-2} \text{d}^{-1}$ determined using the sediment-trap PN flux is almost a factor of 2 higher, $149 \pm 14 \mu\text{mol N m}^{-2} \text{d}^{-1}$. Increasing the water-column ^{234}Th flux by including upwelling increases, the PN export to 98 ± 37 and $124 \pm 47 \mu\text{mol N m}^{-2} \text{d}^{-1}$ for upwelling velocities of 1 and 2 m d^{-1} , respectively. The average PN flux at the OUT stations ranged from $54 \pm 10 \mu\text{mol N m}^{-2} \text{d}^{-1}$ based on water-column ^{234}Th to $160 \pm 22 \mu\text{mol N m}^{-2} \text{d}^{-1}$ using the sediment traps.

The bSiO_2 flux from all five IN stations varied substantially more than either the PC or the PN fluxes due to the rapid change in the $\text{bSiO}_2/^{234}\text{Th}$ ratio with time (Fig. 9). Fluxes of bSiO_2 derived from water-column ^{234}Th and pump $\text{bSiO}_2/^{234}\text{Th}$ ratios ranged from a minimum of $33 \pm 20 \mu\text{mol Si m}^{-2} \text{d}^{-1}$ at station IN-4 to a maximum of $309 \pm 73 \mu\text{mol Si m}^{-2} \text{d}^{-1}$ just 1 day later at station IN-5, immediately following the crash in the diatom bloom. The average bSiO_2 flux for all IN stations was $145 \pm 110 \mu\text{mol Si m}^{-2} \text{d}^{-1}$, a factor of 4 less than that measured directly in the sediment traps, $427 \pm 34 \mu\text{mol Si m}^{-2} \text{d}^{-1}$, but almost 60% higher than the $116 \pm 59 \mu\text{mol Si m}^{-2} \text{d}^{-1}$ determined using a sediment-trap $\text{bSiO}_2/^{234}\text{Th}$ ratio (Fig. 10). Unlike PC and PN, inclusion of an upwelling term did not close the gap, and bSiO_2 fluxes remained a factor of 2 lower than the sediment trap estimates at 215 ± 127 and $267 \pm 159 \mu\text{mol Si m}^{-2} \text{d}^{-1}$ for upwelling rates of 1 and 2 m d^{-1} , respectively. This may be partly due to timescale, as ^{234}Th -based bSiO_2 fluxes at the eddy center are averaged from day 1 to day 6 (no day 2 data available), while the sediment-trap-derived fluxes are integrated from day 2 to day 7 and there is an increase in bSiO_2 fluxes towards the end of the time-series after day 4 (Fig. 9). Some of this difference also may be due to a missing NSS component towards the end of the time-series that remains poorly quantified. The OUT stations, however, show a smaller difference between trap-derived and water-column ^{234}Th -derived bSiO_2 flux estimates relative to the PC and PN fluxes, 111 ± 64 and $100 \pm 13 \mu\text{mol Si m}^{-2} \text{d}^{-1}$, respectively.

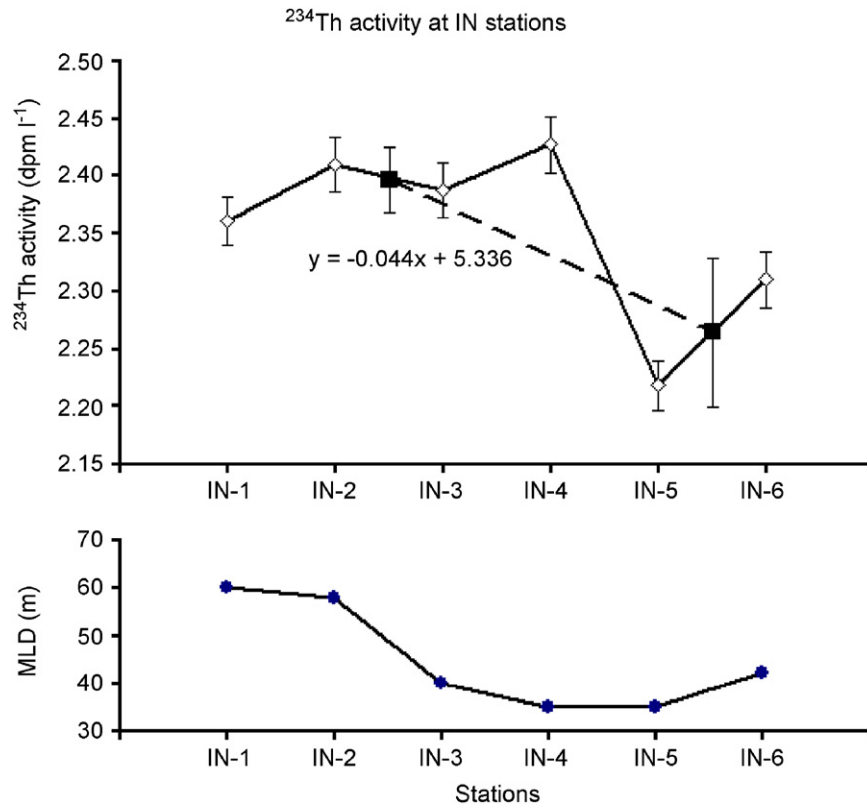


Fig. 6. Integrated ²³⁴Th activity over 0–150 m for IN-1 to IN-6. Black squares represent the average ²³⁴Th activity over IN-1 to IN-4 and IN-5 to IN-6. The change of ²³⁴Th activity over time is calculated to be $-0.044 \text{ dpm L}^{-1} \text{ d}^{-1}$.

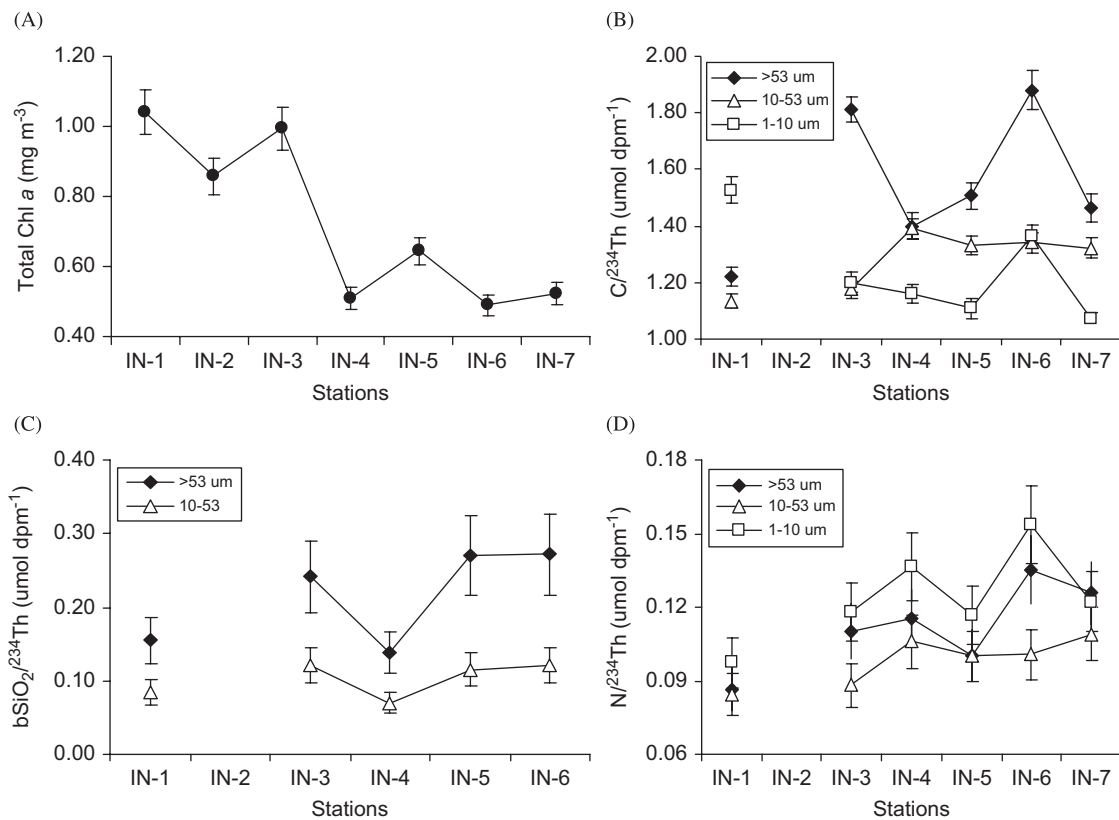


Fig. 7. Temporal variability within Cyclone Opal of (A) total chl a concentrations at the IN stations in the DCML (Rii et al., 2008), (B) PC/²³⁴Th at 150 m, (C) bSiO₂/²³⁴Th at 150 m, and (D) PN/bSiO₂ at 150 m.

Table 2
PC/²³⁴Th, PN/²³⁴Th and bSiO₂/²³⁴Th ratios of samples from the *in situ* pumps

Station type	Filter (μm)	PC/ ²³⁴ Th (μmol dpm ⁻¹)	Error (±) (μmol dpm ⁻¹)	PN/ ²³⁴ Th (μmol dpm ⁻¹)	Error (±) (μmol dpm ⁻¹)	bSiO ₂ / ²³⁴ Th (μmol dpm ⁻¹)	Error (±) (μmol dpm ⁻¹)
Center							
IN-1	53	1.22	0.03	0.09	0.01	0.15	0.03
	10	1.13	0.02	0.08	0.01	0.08	0.02
	1	1.53	0.05	0.10	0.01		
IN-3	53	1.81	0.04	0.11	0.01	0.24	0.05
	10	1.18	0.03	0.09	0.01	0.12	0.02
	1	1.20	0.04	0.12	0.01		
IN-4	53	1.40	0.04	0.11	0.01	0.14	0.03
	10	1.39	0.04	0.11	0.01	0.07	0.01
	1	1.16	0.03	0.14	0.01		
IN-5	53	1.51	0.04	0.10	0.01	0.27	0.05
	10	1.33	0.03	0.10	0.01	0.11	0.02
	1	1.11	0.03	0.12	0.01		
IN-6	53	1.88	0.07	0.13	0.01	0.27	0.05
	10	1.34	0.04	0.10	0.01	0.12	0.02
	1	1.36	0.04	0.15	0.02		
IN-7	53	1.46	0.05	0.13	0.01	0.27	0.05
	10	1.32	0.04	0.11	0.01	0.11	0.04
	1	1.07	0.03	0.12	0.01		
Average IN	53	1.55	0.27	0.11	0.02	0.22	0.06
	10	1.28	0.10	0.10	0.01	0.10	0.02
	1	1.24	0.17	0.12	0.02		
Sediment-trap		1.50	0.04	0.14	0.01	0.40	0.02
Transect 2							
EF-97	53	1.97	0.06	0.15	0.02	0.33	0.07
	10	1.09	0.03	0.09	0.01	0.08	0.02
	1	1.25	0.03	0.13	0.01		
EF-99	53	1.37	0.04	0.09	0.01	0.12	0.02
	10	1.59	0.04	0.14	0.01	0.06	0.01
	1	1.80	0.05	0.24	0.02		
EF-101	53	1.14	0.03	0.08	0.01	0.10	0.02
	10	0.60	0.01	0.05	0.01	0.02	0.01
	1	1.93	0.06	0.25	0.03		
EF-103	53	1.39	0.05	0.12	0.01	0.10	0.02
	10	1.37	0.04	0.13	0.01	0.08	0.01
	1	2.32	0.07	0.37	0.04		
OUT							
OUT-1	53	1.45	0.05	0.12	0.01	0.17	0.03
	10	1.63	0.05	0.13	0.01	0.13	0.03
	1	1.49	0.04	0.21	0.02		
OUT-2	53	1.59	0.06	0.11	0.01	No Data	
	10	1.63	0.05	0.15	0.02	No Data	
	1	1.27	0.03	0.15	0.01		
OUT-3	53	1.77	0.09	0.08	0.01	0.21	0.04
	10	1.35	0.04	0.13	0.01	0.10	0.02
	1	1.69	0.05	0.19	0.02		
Average OUT	53	1.61	0.16	0.10	0.02	0.19	0.02
	10	1.54	0.16	0.14	0.02	0.12	0.02
	1	1.48	0.21	0.18	0.03		
Sediment-trap		2.69	0.09	0.28	0.01	0.20	0.01

Note that no pump samples were collected at IN-2.

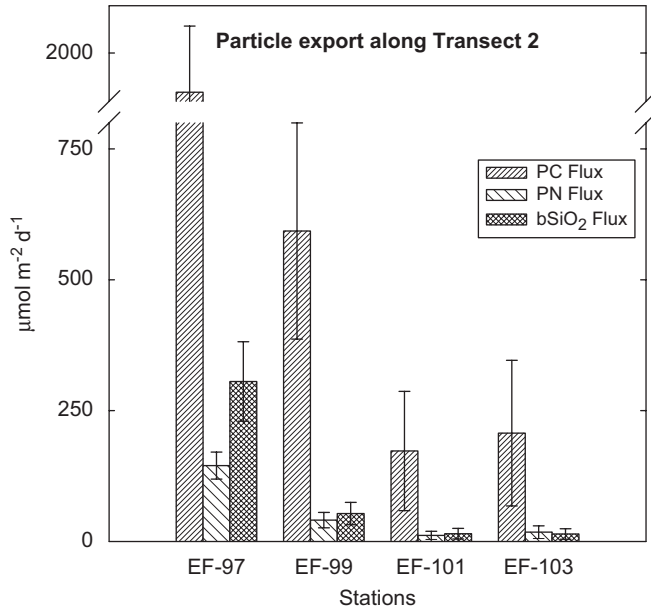


Fig. 8. Observed PC, PN, and bSiO₂ fluxes derived using a SS ²³⁴Th model along Transect 2 measured at 150 m.

4. Discussion

4.1. Biological composition of Cyclone Opal

Mesoscale eddies are dynamic features that may undergo rapid biological evolution (community composition, size structure and trophic interactions) over time (Falkowski et al., 1991; Allen et al., 1996; McGillicuddy and Robinson, 1997; Dickey et al., 1998). This in turn may drive the magnitude and composition of the particle flux (Sweeney et al., 2003; McGillicuddy et al., 2007). In this study, we had the opportunity to examine the composition and flux of particles from a large wind-driven cold-core eddy, Cyclone *Opal*, during the decay of a massive diatom bloom (Rii et al., 2008; Landry et al., 2008a; Brown et al., 2008). Cyclone *Opal* first appeared in satellite imagery between February 18 and 25, 2005, indicating that it was least 4–5 weeks old by the time of our study period.

The biological community within the core of Cyclone *Opal* was vertically heterogeneous. The upper mixed layer (~40 m) was dominated by the cyanobacteria, *Prochlorococcus* and *Synechococcus* spp. (0.2–2 μm in size), similar to that of surrounding waters. Chl *a* concentrations were only slightly elevated (Brown et al., 2008). Growth rates of *Prochlorococcus* spp., and other small phytoplankton, such as prymnesiophytes and pelagophytes, however, were significantly elevated by a factor of two. Just below the depth of the mixed layer (50–60 m), low diatom growth rates were consistent with the observation of senescent diatoms and empty frustules (Brown et al., 2008). Microzooplankton grazing rates remained in balance with diatom growth throughout the upper 60 m (Landry et al., 2008a).

Within the DCM (60–80 m), initial sampling showed the presence of large chain-forming diatoms comprising ~80% of a total biomass that was 100 times greater than surrounding waters (Brown et al., 2008). More than 50% of this diatom biomass was due to diatoms >18 μm in diameter based on size-fractionated pigment analyses (Rii et al., 2008). During the course of the 7-day time-series sampling, however, daily observations of the DCM showed a 80% decrease in diatom biomass and a 70% decrease in the diatom biomarker, fucoxanthin beginning on day 3 (Rii et al., 2008). Total chl *a* concentrations decreased from over 1 to 0.5 mg m^{-3} on day 4 (Fig. 6A, Rii et al., 2008). During this period,

Table 3

Measured and modeled particle fluxes for all stations

Station	Upwelling rate (m d^{-1})	PC flux ($\mu\text{mol C m}^{-2} \text{d}^{-1}$)	PN flux ($\mu\text{mol N m}^{-2} \text{d}^{-1}$)	bSiO ₂ flux ($\mu\text{mol Si m}^{-2} \text{d}^{-1}$)
Center				
IN-1	0	645 ± 170	46 ± 13	82 ± 27
	1	1270 ± 335	90 ± 25	162 ± 53
	2	1895 ± 335	135 ± 38	241 ± 80
IN-3	0	750 ± 267	46 ± 17	100 ± 41
	1	940 ± 335	57 ± 21	126 ± 51
	2	1131 ± 402	69 ± 25	151 ± 62
IN-4	0	332 ± 196	27 ± 16	33 ± 20
	1	817 ± 483	67 ± 40	81 ± 50
	2	1301 ± 769	107 ± 64	129 ± 80
IN-5	0	1719 ± 217	114 ± 18	309 ± 73
	1	2443 ± 308	163 ± 26	439 ± 103
	2	3167 ± 300	211 ± 34	569 ± 134
IN-6	0	1396 ± 281	100 ± 22	202 ± 57
	1	1502 ± 302	108 ± 24	218 ± 62
	2	1608 ± 324	116 ± 26	233 ± 68
Sediment-trap	3	1714 ± 345	123 ± 28	248 ± 70
		1544 ± 112	149 ± 14	427 ± 34
	Transect 2			
EF-97	0	1837 ± 274	145 ± 26	306 ± 76
EF-99	0	593 ± 207	41 ± 15	53 ± 21
EF-101	0	173 ± 114	12 ± 8	15 ± 9
EF-103	0	207 ± 139	18 ± 11	14 ± 9
OUT				
OUT-1	0	764 ± 241	63 ± 21	91 ± 34
OUT-2	0	839 ± 265	56 ± 18	No data
OUT-3	0	933 ± 297	43 ± 14	109 ± 41
Sediment-trap		1522 ± 201	160 ± 22	111 ± 64

the diatom assemblage transitioned from larger centric diatoms, *Chaetoceros* and *Rhizosolenia* genera to lightly silicified *Hemialius* and *Mastogloia*, and there was a relative increase in smaller autotrophs, particularly *Prochlorococcus* spp. (Rii et al., 2008; Brown et al., 2008). The decline in diatom biomass was mainly attributed to the drawdown of silicic-acid below detection limits at the eddy center (Rii et al., 2008).

Large (>50 μm) ciliates and heterotrophic dinoflagellates were nearly three times higher than ambient biomass levels within the DCM (Landry et al., 2008a). Mesozooplankton biomass (>0.2 mm) was significantly elevated within Cyclone *Opal* by a factor of ~1.8 with the majority of mesozooplankton grazing occurring in the smaller size classes (0.2–2 mm) (Landry et al., 2008b). We should note here that it is possible that some of the observed temporal variability in biological community may have been due to patchiness in sampling, even though great care was taken to stay within the eddy center (Nencioli et al., 2008).

4.2. Estimate of particle fluxes

In order to characterize the impact of Cyclone *Opal*'s high biomass, production, and community structure on particle export,

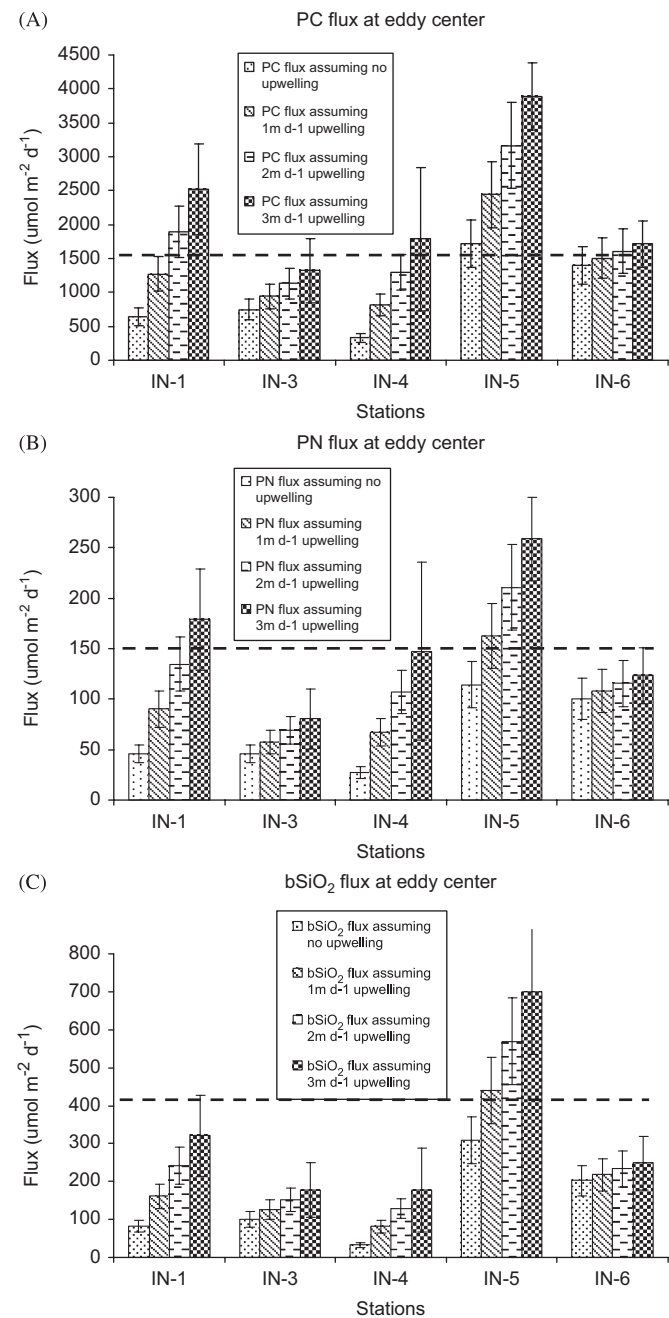


Fig. 9. ^{234}Th -based (A) PC fluxes, (B) PN fluxes, and (C) bSiO₂ fluxes at the center of Cyclone Opal calculated using a SS model and upwelling rates of 0–3 m d⁻¹ and ^{234}Th fluxes measured directly in sediment traps. The dashed lines indicate the sediment-trap-based flux estimates.

we used ^{234}Th measurements in combination with several models that included the effects of physical upwelling and non-steady state processes, as well as collection method (e.g., sediment-trap versus water-column ^{234}Th : ^{238}U disequilibria). Our results suggest that, within the eddy core, ^{234}Th fluxes determined using a SS model with a 2 m d⁻¹ upwelling rate, generally best match the sediment-trap-based ^{234}Th flux measurements. It must be noted, however, that the accuracy of the particle flux is still in question as both sediment traps and ^{234}Th -based methods have their limitations. The assumption of SS is likely invalid, particularly towards the end of the time-series sampling. Large errors associated with the NSS term, however, precluded further use in this study. Inclusion of an upwelling term, provides a better

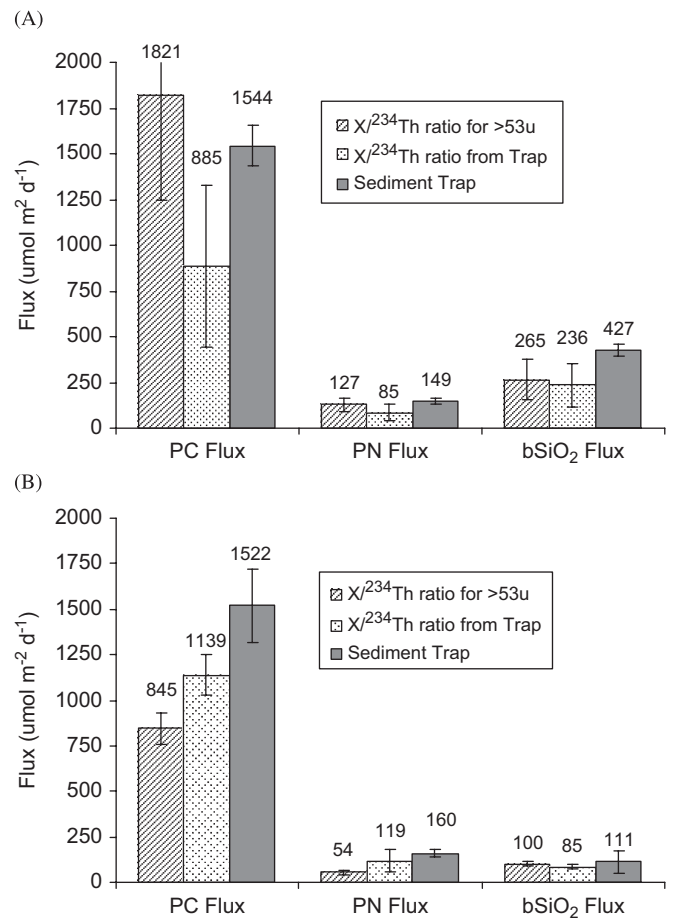


Fig. 10. Average PC, PN and bSiO₂ fluxes derived using a SS ^{234}Th model and upwelling rates of 2 m d⁻¹ at (A) IN stations and (B) OUT stations using PC (PN and bSiO₂/ ^{234}Th) ratios measured in sediment traps and the $\geq 53\text{-}\mu\text{m}$ fraction of the large-volume pump samples.

comparison to ^{234}Th fluxes determined using sediment traps, but it is likely that applying a constant upwelling parameter throughout the time-series is inappropriate. Upper-ocean sediment traps, on the other hand, suffer from a range of collection and sampling biases (Buesseler, 1991; Buesseler et al., 2007). In fact, ^{234}Th fluxes derived using a SS model without upwelling are consistently a factor of 2 lower than that determined from the sediment traps at both IN and OUT stations.

Here, we will use the average of the SS upwelling-derived ^{234}Th flux (assuming 2 m d⁻¹ upwelling) and the ^{234}Th measured using the sediment traps as a reasonable upper estimate of the particle flux within the core of Cyclone Opal. It should be recognized that for each transect and OUT station, only the SS model could be applied. Using this rationale, average PC, PN and bSiO₂ fluxes at the eddy center are $1682 \pm 138 \mu\text{mol C m}^{-2} \text{d}^{-1}$, $138 \pm 11 \mu\text{mol N m}^{-2} \text{d}^{-1}$ and $346 \pm 81 \mu\text{mol Si m}^{-2} \text{d}^{-1}$, respectively (Fig. 9). Average PC, PN and bSiO₂ fluxes measured at the OUT stations were $1185 \pm 478 \mu\text{mol C m}^{-2} \text{d}^{-1}$, $107 \pm 75 \mu\text{mol N m}^{-2} \text{d}^{-1}$, and $106 \pm 10 \mu\text{mol C m}^{-2} \text{d}^{-1}$ respectively, similar to those measured at HOT (Benitez-Nelson et al., 2001). There are no significant differences in PC ($p > 0.66$) and PN ($p > 0.80$) fluxes inside versus outside the eddy; however, bSiO₂ fluxes are elevated by a factor of three within the eddy core ($p < 0.05$). Most of this flux difference is driven by differences in the bSiO₂/ ^{234}Th ratios at IN versus OUT stations (Table 2).

Closer inspection of the PC/ ^{234}Th ratios within Cyclone Opal suggests that, while lower than those observed at HOT

(Benitez-Nelson et al., 2001), these ratios are similar to those determined from the Equatorial Pacific, which also has a diatom-dominated community structure (Buesseler et al., 1995). Low PC/bSiO₂ ratios are also consistent with efficient zooplankton grazing of highly silicified larger centric diatoms, *Chaetoceros* and *Rhizosolenia*, within Cyclone *Opal* and microscopic images of generally empty, but intact diatom frustules within the sediment-trap material (Benitez-Nelson et al., 2007; Rii et al., 2008). These results are similar to Buesseler et al. (2008), who measured ²³⁴Th:²³⁸U disequilibria in the Sargasso Sea mesoscale eddies and found a two- to three-fold increase in bSiO₂ flux without an associated increase in the flux of PC. Note that outside Cyclone *Opal*, PC/bSiO₂ ratios measured at 150 m are significantly higher, consistent with a much lower percentage of diatoms within the overlying planktonic community and a diatom assemblage dominated by lightly silicified *Hemialius* and *Mastogloia* genera typical of oligotrophic waters in the North Pacific Subtropical Gyre (Brown et al., 2008).

4.3. Decoupling of PC and bSiO₂ export

As stated earlier, diatoms comprised more than 80% of the phytoplankton biomass within the eddy core during initial sampling. Two large centric diatom genera, *Rhizosolenia* and *Chaetoceros*, accounted for 35–45% of the diatom biomass, with the remaining assemblage composed of a variety of pennate and large chain-forming centric species (>20 μm). By the end of the bloom, DCM phytoplankton (and diatom) concentrations had decreased by 80% to almost ambient conditions with a transition in diatom species to those more typical of the subtropical North Pacific, such as lightly silicified *Hemiaulus* and *Mastogloia* spp.

Diatoms are often thought to contribute disproportionately to PC flux from surface waters, due to their large size and rapid sinking speeds (Buesseler et al., 1998; Moore et al., 2004; Boyd and Newton, 1995; Michaels and Silver, 1988). Therefore, a lack of a significant eddy-induced increase in PC and PN export was somewhat surprising, as Cyclone *Opal* was a physically well-developed feature, characterized by a transitioning diatom community at the eddy core (Brown et al., 2008; Landry et al., 2008a, b). There are several scenarios that may account for the lack of PC and PN export, while simultaneously enhancing the flux of bSiO₂. The most likely explanation is a tight coupling between protozoan grazing and diatom production (Landry et al., 2008a). A number of studies suggest that protozoa may graze heavily upon diatoms (Buck and Newton, 1995; Landry et al., 2000; Brown et al., 2002). Within Cyclone *Opal*, large (>50 μm) ciliates and heterotrophic dinoflagellates, the most likely grazers of diatoms in the microzooplankton size fraction, were a factor of three greater within the eddy core at the DCM than surrounding waters (Landry et al., 2008a). These organisms capture, consume and process their food as individual prey items, thus producing individual empty frustules as a by-product of grazing (Jacobson and Anderson, 1996; Jeong et al., 2004) as opposed to large organically dense fecal pellets of metazooplankton grazers or the mass settling of intact cells as aggregates (e.g., Sarthou et al., 2005). As a result, protozoan feeding on diatoms produce Si-rich, C-poor sinking material. In fact, there were relatively few fecal pellets observed in the sediment-trap material at either IN or OUT stations (Susan Brown, personal communication). Mesozooplankton biomass was also significantly elevated within Cyclone *Opal* with the majority of mesozooplankton grazing occurring in the smaller size classes (Landry et al., 2008b). As a result, Landry et al. (2008b) suggested that at least some of their egested material sank slowly, and was degraded and recycled within the euphotic zone (e.g., Paffenhoefer and Knowles, 1979; Hofmann et al., 1981).

The abundance of senescent, or “empty diatom” cells within the upper water-column of Cyclone *Opal* indicates that these cells may have “leaked carbon” as the population became nutrient stressed (Brown et al., 2008; Benitez-Nelson et al., 2007). This theory is corroborated by the large accumulation of dissolved organic C (DOC) in the euphotic zone, which accounts for >85% of the new production estimated to occur within the eddy core (Benitez-Nelson et al., 2007). The increase in DOC also points to selective remineralization and temperature-dependent interactions between senescent diatom cells and bacteria (Ragueneau et al., 2006), which may result in a decoupling between C and Si remineralization as well. Viruses were not studied during this cruise and they may also play an important role in emptying diatoms through viral lysis (Fuhrman, 1999).

Enhanced bSiO₂ fluxes are further consistent with observations of Ingalls et al. (2006), who suggested that organic matter in diatom rich regions are more heavily processed by zooplankton, and thus can potentially export a higher proportion of silica as highly silicified empty frustules that contain relatively less organic matter. This is also in agreement with current knowledge of the organic matter carrying capacity of different ballast types, as it is suggested that in general, calcium carbonate carries the largest loading of organic matter, while opal carries the smallest (Klaas and Archer, 2002).

4.4. Export efficiency

PP was determined from growth rate measurements at all process stations (Benitez-Nelson et al., 2007; Landry et al., 2008a). Within the eddy core, 0–110 m integrated PP rates ranged from a high of 124 mmol m⁻² d⁻¹ at the beginning of the time-series occupation, to a low of 34 mmol m⁻² d⁻¹ after the crash of the diatom bloom. At the OUT stations, PP rates integrated over the upper 150 m averaged 27 ± 9 mmol m⁻² d⁻¹. No correlation between PP and ²³⁴Th-derived PC export was observed. A similar lack of correlation between PP and PC export has been reported for station ALOHA (Benitez-Nelson et al., 2001; Karl et al., 1996) and the Bermuda Atlantic Time-series station (BATS, Michaels and Knap, 1996). It is likely related to temporal differences in the factors that contribute to PP (e.g., nutrients and light) versus export (community structure and grazing) (Benitez-Nelson et al., 2001). Another possibility may be due to the spatial variability associated with the two sampling methods: while sediment traps integrate over a large region, PP is usually calculated from a single water-column profile.

Using PP and measured PC fluxes, the export ratio (PC export to PP) can be estimated, i.e., the percentage of PP that is exported to depth as sinking particles. The average export efficiency for IN stations is 2.7%. The average export efficiency for the OUT stations is 4.3%. Thus, despite the large increase in PP within Cyclone *Opal*, the export ratio is still similar to surrounding waters and other oligotrophic regions of the world oceans, including HOT and BATS (~5%) (Buesseler, 1998; Benitez-Nelson et al., 2001). ²³⁴Th fluxes within Cyclone *Opal* are also consistent with the magnitude and *f*-ratio of a previously studied, older Hawaiian Cyclone, *Haulani*, which showed a particulate ²³⁴Th export of ~1100 dpm m⁻² d⁻¹, enhanced PC export by a factor of 2.6, and an *f*-ratio of 3.5% (Bidigare et al., 2003). The low export-ratios suggest that although Cyclone *Opal* was dominated by large, presumably rapidly sinking diatoms, the eddy was highly inefficient in the transport of PC to depth, consistent with results from the Southern Ocean Iron Experiment (SOFEX) (Buesseler et al., 2005), direct measurements of particle export in mesoscale eddies in the Sargasso Sea (Buesseler et al. 2008), and a recent study by Richardson and

Jackson (2007) that diatoms do not disproportionately contribute to particle flux in open-ocean systems.

4.5. Shallow depth of PC and PN remineralization

Low export ratios within Cyclone *Opal* suggest efficient particle remineralization and accumulation of DOC and suspended PC from surface waters. Anecdotal evidence already suggests that remineralization is an important process within the eddy as particle export is dominated by empty diatom frustules within the euphotic zone rather than organically rich, rapidly sinking particle aggregates, such as fecal pellets. Closer inspection of water-column ^{234}Th depth profiles confirms important PC remineralization trends. When ^{234}Th concentrations are in excess of ^{238}U activities, remineralization or accumulation of dissolved and suspended PC must have occurred. This is clearly shown by $^{234}\text{Th}/^{238}\text{U}$ distributions observed during the IN station sampling, with a zone of intense particle scavenging, $^{234}\text{Th}/^{238}\text{U} < 1$, throughout the upper 100 m, underlain by a region of rapid remineralization from 100 to 175 m (Fig. 11). The remineralization peaks are more intense and shallower than those observed in the surrounding waters, including HOT (Benitez-Nelson et al., 2001). For stations along Transect 1 and the OUT stations, a large excess in ^{234}Th activity is generally found within the 150–200 m horizon, whereas deficiencies, e.g., particle scavenging, generally occur in the overlying 100–150 m. The IN stations, however, show an excess or very small deficiency in ^{234}Th activity for the 100–175 m interval (except for IN-5) indicating that maximum remineralization takes place at shallower depths, with a large fraction above the 150-m depth horizon used to determine particle flux in this study. Similar layers of shallow remineralization peaks in ^{234}Th profiles are also found to be associated with eddies in the Sargasso Sea (Buesseler et al., 2008) and are attributed to rapid remineralization and particle break up.

Shallow PC and PN remineralization depths are further supported by the composition of bacterial community. Bacterioplankton communities in the mixed layer above 50 m were similar to those measured outside the eddy. Below 50 m, however, there appeared Planctomycetes, Bacteroidetes and Proteobacteria phyla, which are frequently found associated with marine

particulate matter and hypothesized to degrade high molecular-weight organic matter (Benitez-Nelson et al., 2007).

Sweeney et al. (2003) proposed a conceptual model of the effects of mode-water and cyclonic eddies on the upper ocean ecosystem. They suggested seven stages within an eddy life cycle corresponding to eddy intensification or spin-up (stages 1–2 dominated by nutrient injection), maturity (stages 3–5, dominated by a biological response with export towards the latter stages), and decay or relaxation (stages 6–7, dominated by particle export). The large decrease in PP rates coupled with the rapid change in community structure all suggest that this eddy was in the mature to decay phase (stages 4–6). It is possible that our particle export sampling may have occurred too early, or that we may have missed the major export event. However, several lines of evidence contradict the latter theory. ^{234}Th export fluxes integrate over the preceding 4–6 weeks. Additional measurements of ^{210}Po , which integrates over several-month time scales, also find similar results (Verdeny et al., 2008). Mass balance estimates of DOC within Cyclone *Opal* suggest that more than 85% of net community production accumulated in the upper 110 m as DOC rather than exported as PC (Benitez-Nelson et al., 2007). In addition, ^{234}Th , ^{210}Po and sediment-trap results from an older, later stage eddy, Cyclone *Noah*, showed little to no enhanced export (Maiti, unpublished results, Rii et al., 2008, Verdeny et al., 2008). Hence, our results are contrary to the hypothesis that a mature stage of an eddy should be associated with higher particle export. Instead, mechanisms of nutrient injection and rapid changes in community structure also must be considered.

5. Conclusions and significance

^{234}Th depth profiles suggest that much of Cyclone *Opal*'s particle production occurred in the upper 100 m, and was rapidly remineralized by 150 m to the suspended and dissolved phase. As a result, increased fluxes of PC and PN expected from the large increase in PP and large diatom growth did not occur. Rather, export was dominated by empty silica frustules that appeared to have been grazed upon by microzooplankton. The surprising low export efficiency inside the eddy is consistent with recent models

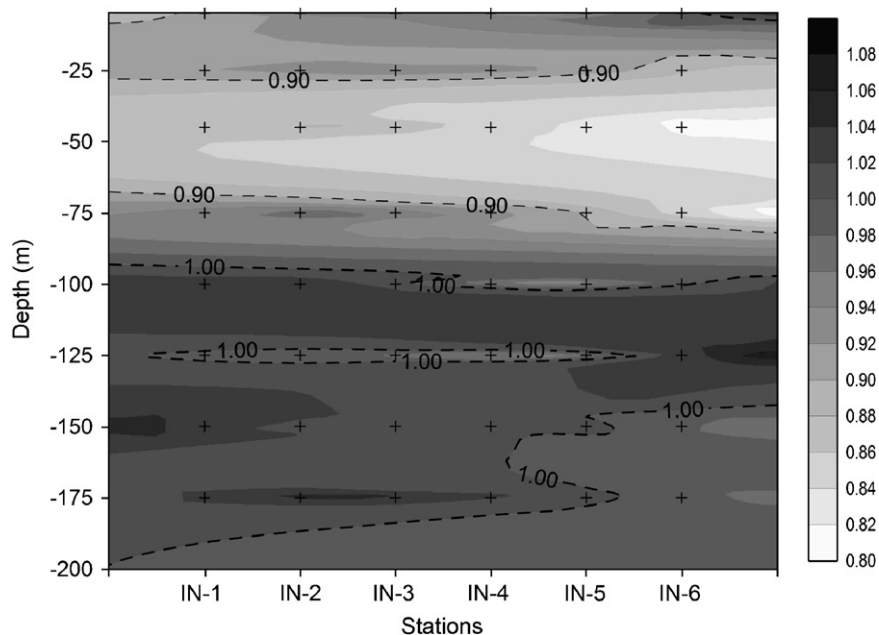


Fig. 11. Contour plot of the $^{234}\text{Th}/^{238}\text{U}$ ratio for the six IN stations. Note that each station represents exactly 1 d (± 1 h).

of the role of temperature on export production, such as Laws et al. (2000) pelagic food web model, as well as warm-water diatom blooms induced by iron fertilization in the Equatorial Pacific. Laws et al. (2000) suggest that at temperature ≥ 25 °C *f*-ratios are low at all rates of production. According to the model, *f*-ratios are only sensitive to production at low to moderate rates of production and at temperature < 25 °C.

This study confirms that wind-driven eddies can be highly productive and can increase both biomass and particle flux, but they are not necessarily more efficient in exporting PC and PN to deeper waters. In fact, they are more effective as “silica pump”. While it is difficult to expand this conclusion to other sites, and other types of eddies, we should note that eddy-induced particle export rates determined here are similar to those that have been measured in mode water and cyclonic eddies in the Sargasso Sea (Sweeney et al., 2003). In order to obtain a larger scale estimate of the role of cyclonic eddies in PC and bSiO₂ export in this region, we made some simple calculations. Lumpkin (1998) determined that on average nine cyclonic eddies occur each year in the lee of the Hawaiian Islands, with one eddy per month generated during the winter months over the 3-year period from 1993 to 1995. These eddies had spin-up periods averaging 5–20 days and lifetimes of 3–8 months. By using the annual average of nine cyclonic eddies and assuming each eddy lasts ~ 7 days in its mature stage, and maintains a export core of just 40 km (from this study), we estimate that the total PC and bSiO₂ export to be 13.3×10^7 mol C y⁻¹ and 2.7×10^7 mol Si y⁻¹, respectively. For comparison, the total PC and bSiO₂ export that would have taken place if no eddy was present in these waters, i.e., over an area with 40 km diameter (same area as the eddy core) and assuming that they behaved in the same way as the OUT stations, are 7.6×10^7 mol C y⁻¹ and 0.63×10^7 mol Si y⁻¹, respectively (based on our OUT station measurements). While it is difficult to assess the number and spatial extent of eddies in the North Pacific, these speculative results suggest that mesoscale eddies of this type may play an important role in the removal of bSiO₂ in Pacific Ocean waters. Further research must be conducted in order to fully decipher the role of not just cyclonic eddies, but other mesoscale eddies and features that inject nutrients into surface waters.

Acknowledgments

We thank all of our E-Flux collaborators especially Jamie Becker, Paulo Calil and Rob Bidigare for their assistance during sample collection. The crew of the R/V *Wecoma* are thanked for their assistance at sea. CHN analyses were performed with the help of Eric Tappa and the bSiO₂ analyses were carried out by Renee Styles. This study was funded by the National Science Foundation (Chemical Oceanography Grant OCE-0241645).

References

- Allen, C.B., Kanda, J., Laws, E.A., 1996. New production and photosynthetic rates within and outside a cyclonic mesoscale eddy in the North Pacific Subtropical Gyre. *Deep-Sea Research Part I—Oceanographic Research Papers* 43 (6), 917–936.
- Bacon, M.P., Cochran, J.K., Hirschberg, D., Hammar, T.R., Fleer, A.P., 1996. Export flux of carbon at the equator during the EqPac time-series cruises estimated from ²³⁴Th measurements. *Deep-Sea Research I* 48, 2595–2611.
- Benitez-Nelson, C.R., Charette, M., 2004. Uncertainty versus variability in upper ocean carbon flux estimates. *Limnology and Oceanography* 49 (4), 1218–1220.
- Benitez-Nelson, C., Buesseler, K.O., Karl, D., Andrews, J., 2001. A time-series study of particulate matter export in the North Pacific Subtropical Gyre based upon ²³⁴Th/²³⁸U disequilibrium. *Deep-Sea Research I* 48, 2595–2611.
- Benitez-Nelson, C., Bidigare, R., Dickey, T., Landry, M., Leonard, C., Brown, S., Nencioli, F., Rii, Y., Maiti, K., Becker, J. Bibby, T., Black, W., Cai, W., Carlson, C., Chen, F., Kuwahara, V., Mahaffey, C., McAndrew, P., Quay, P., Rappé, Selph, K., Simmons, M., Yang, E., 2007. Mesoscale eddies drive increased silica export in the subtropical Pacific Ocean. *Science* 312, 1017–1021.
- Bidigare, R.R., Benitez-Nelson, C.R., Leonard, C.L., Quay, P., Parsons, M.L., Foley, D.G., Seki, M.P., 2003. Influence of a cyclonic eddy on microheterotroph biomass and carbon export in the lee of Hawaii. *Geophysical Research Letters* 30 (6), 1318.
- Boyd, P.W., Newton, P.P., 1995. Evidence of potential influence of planktonic community structure on the interannual variability of particulate organic carbon flux. *Deep-Sea Research I* 42, 619–639.
- Brown, S.L., Landry, M.R., Christensen, S., Garrison, D., Gowing, M.M., Bidigare, R.R., Campbell, L., 2002. Microbial community dynamics and taxon-specific phytoplankton production in the Arabian Sea during the 1995 monsoon seasons. *Deep-Sea Research Part II: Topical Studies in Oceanography. The 1994–1996 Arabian Sea Expedition: Oceanic Response to Monsoon al Forcing, Part 5*, 49(12), 2345–2376.
- Brown, S.L., Landry, M.R., Selph, K.E., Yange, E.J., Rii, Y.M., Bidigare, R.R., 2008. Diatoms in the desert: Plankton community response to a subtropical mesoscale eddy in the subtropical North Pacific. *Deep-Sea Research II*, this issue [doi:10.1016/j.dsr2.2008.02.012].
- Buck, K.R., Newton, J., 1995. Fecal pellet flux in Dabob Bay during a diatom bloom: contribution of microzooplankton. *Limnology and Oceanography* 40, 306–315.
- Buesseler, K.O., 1991. Do upper-ocean sediment traps provide an accurate record of particle flux? *Nature* 353, 420–423.
- Buesseler, K.O., 1998. The decoupling of production and particulate export in the surface ocean. *Global Biogeochemical Cycles* 12, 297–310.
- Buesseler, K.O., Bacon, M.P., Cochran, J.K., Livingston, H.D., 1992. Carbon and nitrogen export during the JGOFS North-Atlantic bloom experiment estimated from Th-234:U-238 disequilibrium. *Deep-Sea Research Part a—Oceanographic Research Papers* 39 (7–8A), 1115–1137.
- Buesseler, K.O., Andrews, J.A., Hartman, M.C., Belostock, R., Chai, F., 1995. Regional estimates of the export flux of particulate organic carbon derived from thorium-234 during the JGOFS EqPac program. *Deep-Sea Research II* 42 (2–3), 777–804.
- Buesseler, K.O., Ball, L., Andrews, J.A., Benitez-Nelson, C., Belostock, R., Chai, F., Chao, Y., 1998. Upper ocean export of particulate organic carbon in the Arabian Sea derived from thorium-234. *Deep-Sea Research II* 45, 2461–2487.
- Buesseler, K.O., Benitez-Nelson, C.R., Rutgers van der Loeff, M.M., Andrews, J.A., Ball, L., Crossin, G., Charette, M.A., 2001. An intercomparison of small- and large-volume techniques for thorium-234 in seawater. *Marine Chemistry* 74, 15–28.
- Buesseler, K.O., Andrews, J.E., Pike, S., Charette, M.A., Goldson, L.E., Brzezinski, M.A., Lance, V.P., 2005. Particle export during the Southern Ocean Iron Experiment (SOFeX). *Limnology and Oceanography* 50, 311–327.
- Buesseler, K.O., Benitez-Nelson, C.R., Moran, S.B., Burd, A., Charette, M., Cochran, J.K., Coppola, L., Fisher, N.S., Fowler, S.W., Gardner, W.D., 2006. An assessment of particulate organic carbon to thorium-234 ratios in the ocean and their impact on the application of ²³⁴Th as a POC flux proxy. *Marine Chemistry* 100 (3–4), 213–233.
- Buesseler, K.O., Antia, A.N., Chen, M., Fowler, S.W., Gardner, W.D., Gustafsson, O., Harada, K., Michaels, A.F., Rutgers van der Loeff, M., Sarin, M., Steinberg, D.K., Trull, T., 2007. An assessment of the use of sediment traps for estimating upper ocean particle fluxes using sediment traps. *Journal of Marine Research* 65, 345–416.
- Buesseler, K.O., Lamborg, C., Cai, P., Escoube, R., Johnson, R., Pike, S., Masque, P., McGillicuddy, D., Verdeny, E., 2008. Particle fluxes associated with mesoscale eddies in the Sargasso Sea. *Deep-Sea Research II*, this issue [doi:10.1016/j.dsr2.2008.02.007].
- Chavanne, C., Flamant, P., Lumpkin, R., Dousset, B., Bentamy, A., 2002. Scatterometer observations of wind variations by oceanic islands: implications for wind driven ocean circulation. *Canadian Journal of Remote Sensing* 28 (3), 466–474.
- Chen, J.H., Edwards, R.L., Wasserburg, G.J., 1986. ²³⁸U, ²³⁴U and ²³²Th in seawater. *Earth and Planetary Science Letters* 80, 241–251.
- Cheney, R.E., Richardson, P.L., 1976. Observed decay of a cyclonic Gulf Stream ring. *Deep-Sea Research* 23, 143–155.
- Cochran, J.K., Barnes, C., Achman, D., Hirschberg, D.J., 1995. Thorium-234/Uranium-238 disequilibrium as an indicator of scavenging rates and particulate organic carbon fluxes in the Northeast Water Polynya, Greenland. *Journal of Geophysical Research* 100, 4399–4410.
- DeMaster, D.J., 1981. The supply and accumulation of silica in the marine environment. *Geochimica et Cosmochimica Acta* 45, 1715–1732.
- Dickey, T., Marra, J., Sigurdson, D.E., Weller, R.A., Kinkade, C.S., Zedler, S.E., Wiggert, J.D., Langdon, C., 1998. Seasonal variability of bio-optical and physical properties in the Arabian Sea: October 1994–October 1995. *Deep-Sea Research II* 45, 2001–2025.
- Dickey, T., Nencioli, F., Kuwahara, V., Leonard, C., Black, W., Bidigare, R.R., Rii, Y., Zhang, Q., 2008. Physical and bio-optical observations of oceanic cyclones west of the Island of Hawai'i. *Deep-Sea Research II*, this issue [doi:10.1016/j.dsr2.2008.01.006].
- Dower, J.F., Denman, K.L., 2001. Effects of small-scale physics on plankton biology. In: Steele, J.H., Turekian, K.K., Thorpe, S.A. (Eds.), *The Encyclopedia of Ocean Sciences*. Academic Press, pp. 2834–2839.
- Falkowski, P.G., Ziemann, D.A., Kolber, Z., Bienfang, P.K., 1991. Role of eddy pumping in enhancing primary production in the ocean. *Nature* 352, 55–58.
- Flierl, G., McGillicuddy, D.J., 2002. Mesoscale and submesoscale physical-biological interactions. Chapter 4. In: Robinson, A.R., McCarthy, J.J., Rothschild, B.J. (Eds.), *The Sea*. Wiley, New York, pp. 113–186.

- Fuhrman, J., 1999. Marine viruses and their biogeochemical and ecological effects. *Nature* 399, 541–548.
- Garçon, V.C., Oschlies, A., Doney, S.C., McGillicuddy, D., Waniek, J., 2001. The role of mesoscale variability on plankton dynamics in the North Atlantic. *Deep-Sea Research Part II—Topical Studies in Oceanography* 48 (10), 2199–2226.
- Hansen, A.L., Koroleff, F., 1999. Determination of nutrients. In: Grasshoff, K., Kremling, K., Ehrhardt, M. (Eds.), *Methods of Seawater Analysis*. Wiley-VCH, Weinheim, pp. 159–228.
- Haurly, L.R., 1984. An offshore eddy in the California Current System. Part IV: Plankton distributions. *Progress in Oceanography* 13, 95–111.
- Haurly, L.R., McGowan, J.A., Weibe, P.H., 1978. Patterns and processes in the time-space scales of plankton distributions. In: Steele, J.H. (Ed.), *Spatial Pattern in Planktonic Community*. Plenum, New York, pp. 277–327.
- Hofmann, E., Busalacchi, A., O'Brien, J.J., 1981. Wind generation of Costa Rica Dome. *Science* 214, 552–554.
- Ingalls, A.E., Liu, Z., Lee, C., 2006. Seasonal trends in the pigment and amino acid compositions of sinking particles in biogenic CaCO₃ and SiO₂ dominated regions of the Pacific sector of the Southern Ocean along 170°W. *Deep-Sea Research I* 53, 836–859.
- Jacobson, D.M., Anderson, D.M., 1996. Widespread phagocytosis of ciliates and other protists by marine mixotrophic and heterotrophic thecate dinoflagellates. *Journal of Phycology* 32, 279–285.
- Jeong, H.J., Yoo, Y.D., Kim, S.T., Kang, N.S., 2004. Feeding by the heterotrophic dinoflagellate *Protoperidinium bipes* on the diatom *Skeletonema costatum*. *Aquatic Microbial Ecology* 36, 171–179.
- Karl, D.M., Dore, J.J., Hebel, D.J., Winn, C., 1991. Procedures for particulate carbon, nitrogen, phosphorus and total mass analyses in the US-JGOFS Hawaii Ocean Time-series program. In: Hurd, D., Spencer, D.W. (Eds.), *Marine Particles: Analyses and Characterization*, Geophysical Monograph 63. American Geophysical Union, Washington, DC, pp. 17–71.
- Karl, D.M., Christian, J.R., Dore, J.E., Hebel, D.V., Letelier, R.M., Tupas, L.M., Winn, C.D., 1996. Seasonal and interannual variability in primary production and particle flux at Station ALOHA. *Deep-Sea Research II* 43, 539–568.
- Klaas, C., Archer, D.E., 2002. Association of sinking organic matter with various types of mineral ballast in the deep sea: implications for the rain ratio. *Global Biogeochemical Cycles* 16, 1116.
- Landry, M.R., Constantinou, J., Latasa, M., Brown, S.L., Bidigare, R.R., Ondrusek, M.E., 2000. Biological response to iron fertilization in the eastern equatorial Pacific (IronEx II). III. Dynamics of phytoplankton growth and microzooplankton grazing. *Marine Ecology—Progress Series* 201, 57–72.
- Landry, M.R., Brown, K.E., Selph, K.E., Simmons, M.P., Rii, Y.M., 2008a. Depth-stratified phytoplankton dynamics in Cyclone *Opal*, a subtropical mesoscale eddy. *Deep-Sea Research II*, this issue [doi:10.1016/j.dsr2.2008.02.001].
- Landry, M.R., Decima, M., Simmons, M.P., Hannides, C.C.S., Daniels, E., 2008b. Mesozooplankton biomass and grazing responses to Cyclone *Opal*, a subtropical mesoscale eddy. *Deep-Sea Research II*, this issue [doi:10.1016/j.dsr2.2008.01.005].
- Laws, E.A., Falkowski, P.G., Smith, R.C., Ducklow, H., McCarthy, J.J., 2000. Temperature effects on export production in the open ocean. *Global Biogeochemical Cycles* 14, 1231–1246.
- Letelier, R.M., Karl, D.M., Abbott, M.R., Flament, P., Freilich, M., Lukas, R., Strub, T., 2000. Role of late winter mesoscale events in the biogeochemical variability of the upper water column of the North Pacific Subtropical Gyre. *Journal of Geophysical Research—Oceans* 105 (C12), 28723–28739.
- Lumpkin, C.F., 1998. Eddies and currents of the Hawaiian Islands. Ph.D. Dissertation, University of Hawaii, 281pp.
- McGillicuddy, D.J., Robinson, A.R., 1997. Eddy-induced nutrient supply and new production in the Sargasso Sea. *Deep-Sea Research I* 44, 1427–1449.
- McGillicuddy, D.J., Robinson, A.R., Siegel, D.A., Jannasch, H.W., Johnson, R., Dickey, T., McNeil, J., Michaels, A.F., Knap, A.H., 1998. Influence of mesoscale eddies on new production in the Sargasso Sea. *Nature* 394 (6690), 263–266.
- McGillicuddy, D.J., Anderson, L.A., Bates, N.R., Bibby, T., Buesseler, K.O., Carlson, C.A., Davis, C.S., Ewart, C., Falkowski, P.G., Goldthwait, S.A., Hansell, D.A., Jenkins, W.J., Johnson, R., Kosnyrev, V.K., Ledwell, J.R., Li, Q.P., Siegel, D.A., Steinberg, D.K., 2007. Eddy/wind interactions stimulate extraordinary mid-ocean plankton blooms. *Science* 316, 1021–1026.
- Michaels, A.F., Knap, A.H., 1996. Overview of the US JGOFS Bermuda Atlantic Time-series Study and the Hydrostation S program. *Deep-Sea Research Part II—Topical Studies in Oceanography* 43 (2–3), 157–198.
- Michaels, A.F., Silver, M.W., 1988. Primary production, sinking fluxes and the microbial food web. *Deep-Sea Research* 35, 473–490.
- Moore, J.K., Doney, S.C., Lindsay, K., 2004. Upper ocean ecosystem dynamics and iron cycling in a global three-dimensional model. *Global Biogeochemical Cycles* 18, GB4028, 4010.1029/2004GB002220.
- Murray, J.W., Young, J., Newton, J., Dunne, T., Chapin, B.P., 1996. Export flux of particulate organic carbon from the central equatorial Pacific determined using combined drifting trap ²³⁴Th approach. *Deep-Sea Research II* 43, 1095–1132.
- Nencioli, F., Dickey, T.D., Kuwahara, V.S., Black, W., Rii, Y.M., Bidigare, R.R., 2008. Physical dynamics and biological implications of a mesoscale cyclonic eddy in the lee of Hawaii: Cyclone *Opal* observations during E-Flux III. *Deep-Sea Research II*, this issue [doi:10.1016/j.dsr2.2008.02.003].
- Olaizola, M., Ziemann, D.A., Bienfang, P.K., Walsh, W.A., Conquest, L.D., 1993. Eddy induced oscillations of the pycnocline affect the floristic composition and depth distribution of phytoplankton in the subtropical Pacific. *Marine Biology* 116, 533–542.
- Olson, D.B., 1980. The physical oceanography of two rings observed by the Cyclonic Ring Experiment. Part II: Dynamics. *Journal of Physical Oceanography* 10, 514–527.
- Oschlies, A., Garçon, V., 1998. Eddy-induced enhancement of primary production in a model of the north Atlantic Ocean. *Nature* 394 (6690), 266–269.
- Paffenhofer, G.A., Knowles, S.C., 1979. Ecological implications of fecal pellet size, production and consumption by copepods. *Journal of Marine Research* 37, 35–49.
- Patzel, W.C., 1969. Eddies in Hawaiian waters. HIG Technical Report 69-8, Hawaii Institute of Geophysics, University of Hawaii.
- Pike, S.M., Buesseler, K.O., Andrews, J., Savoye, N., 2005. Quantification of ²³⁴Th recovery in small volume sea water samples by inductively coupled plasma mass spectrometry. *Journal of Radioanalytical and Nuclear Chemistry* 263 (2), 355–360.
- Ragueneau, O., Schultes, S., Bidle, K., Clauquin, P., Moriceau, B., 2006. Si and C interactions in the world ocean: importance of ecological processes and implications for the role of diatoms in the biological pump. *Global Biogeochemical Cycles* 20, GB1013.
- Richardson, T.L., Jackson, G.A., 2007. Small phytoplankton and carbon export from the surface ocean. *Science* 315 (5813), 838–840.
- Rii, Y.M., Brown, S.L., Nencioli, F., Kuwahara, V., Dickey, T., Karl, D.M., Bidigare, R.R., 2008. The transient oasis: nutrient-phytoplankton dynamics and particle export in Hawaiian Lee Cyclones. *Deep-Sea Research II*, this issue [doi:10.1016/j.dsr2.2008.01.013].
- Rutgers van der Loeff, M.R., Sarin, M.M., Baskaran, M., Benitez-Nelson, C., Buesseler, K.O., Charette, M., Dai, M., Gustafsson, O., Masque, P., Morris, P., 2006. A review of present techniques and methodological advances in analyzing ²³⁴Th in aquatic systems. *Marine Chemistry* 100 (3–4), 190–212.
- Sarthou, G., Timmermans, K.R., Blain, S., Treguer, P., 2005. Growth physiology and fate of diatoms in the ocean: a review. *Journal of Sea Research* 53 (1–2), 25–42.
- Savidge, G., Williams, P.J.L., 2001. The PRIME 1996 cruise: an overview. *Deep-Sea Research Part II—Topical Studies in Oceanography* 48 (4–5), 687–704.
- Savoye, N., Benitez-Nelson, C., Burd, A.B., Cochran, J.K., Charette, M., Buesseler, K.O., Jackson, G.A., Roy-Barman, M., Schmidt, S., Elskens, M., 2006. ²³⁴Th sorption and export models in the water column: a review. *Marine Chemistry* 100 (3–4), 234–249.
- Seki, M.P., Polovina, J.J., Brainard, R.E., Bidigare, R.R., Leonard, C.L., Foley, D.G., 2001. Biological enhancement at cyclonic eddies tracked with GOES thermal imagery in Hawaiian waters. *Geophysical Research Letters* 28, 1583–1586.
- Siegel, D.A., McGillicuddy, D.J., Fields, E.A., 1999. Mesoscale eddies, satellite altimetry, and new production in the Sargasso Sea. *Journal of Geophysical Research—Oceans* 104 (C6), 13359–13379.
- Sweeney, E.N., McGillicuddy, D.J., Buesseler, K.O., 2003. Biogeochemical impacts due to mesoscale eddy activity in the Sargasso Sea as measured at the Bermuda Atlantic Time-series Study (BATS). *Deep-Sea Research Part II: Topical Studies in Oceanography The US JGOFS Synthesis and Modeling Project: Phase II* 50 (22–26), 3017–3039.
- van Haren, H., Millot, C., Taupier-Letage, I., 2006. Fast deep sinking in Mediterranean eddies. *Geophysical Research Letters* 33, L04606, 10.1029/2005GL025367.
- Verdeny, E., Masqué, P., Maiti, K., Garcia-Orellana, J., Bruach, J.M., Benitez-Nelson, C.R., 2008. Particle export within cyclonic Hawaiian lee eddies derived from ²¹⁰Pb–²¹⁰Po disequilibria. *Deep-Sea Research II*, this issue [doi:10.1016/j.dsr2.2008.02.009].
- Woods, J.D., 1988. Mesoscale upwelling and primary production. In: Rothschild, B.J. (Ed.), *Towards a Theory on Biological–Physical Interactions in the World Ocean*. Kluwer, pp. 7–38 NATO ASI Series.